EDGE ARTICLE

Check for updates

Synthesis of perhalogenated silylboranes (X = Cl, I) and their application in regiodivergent alkene silaboration

Jan Heller,[†][a] Christoph D. Buch,[†][a] Alexander V. Virovets, [ID][a] Eugenia Peresypkina, [ID][a] Hans-Wolfram Lerner, [ID][a] Felipe Fantuzzi [ID][b] and Matthias Wagner *[a]

Silaboration of olefins is a synthetically valuable and atom-economic mode of functionalization; however, it typically requires transition-metal catalysis. We have overcome this requirement by using highly reactive perhalogenated silylboranes, $X_2B–SiX_3$ (X = Cl, I), for which we herein report a straightforward synthesis, a full characterization, and their key properties. Access to this compound class was enabled by substantial improvement in the synthesis protocol for our previously published compound $[Et_4N][I_3B–SiI_3]$, now available on a 40 g scale *via* only two steps. Cation exchange with $Li[Al(OC(CF_3)_3)_4]$ affords the mixture $Li[I_3B–SiI_3]/I_2B–SiI_3/LiI$, serving as a synthetic equivalent of the elusive pure $I_2B–SiI_3$. Its chlorine analogue $Cl_2B–SiCl_3$ is accessible as a distillable liquid *via* treatment of $[Et_4N][I_3B–SiI_3]$ with $GaCl_3$. For both perhalogenated silylboranes, various Lewis base adducts $Do·X_2B–SiX_3$ were obtained in excellent yields and structurally characterized by X-ray diffraction (Do = SMe_2, Py, PPh_3, IDipp; IDipp = 1,3-bis(2,6-diisopropylphenyl)-1,3-dihydro-2*H*-imidazol-2-ylidene). We demonstrated that $Me_2S·I_2B–SiI_3$ undergoes efficient 1,2-silaboration of the challenging, non-activated substrate ethylene at rt with 0.1 eq. BI_3 as promoter. In contrast, $Li[I_3B–SiI_3]/I_2B–SiI_3/LiI$ effects a quantitative, unprecedented 1,1-silaboration of cyclohexene at rt. This remarkable reactivity switch was elucidated by experimental and quantum-chemical studies of the underlying steric and electronic factors.

Introduction

Once considered exotic and of limited utility, perhalogenated diborane(4) and disilane compounds (**I**, **III**; Fig. 1a) have recently emerged as valuable building blocks for purposes ranging from organic synthesis to materials development.[1–6] The direct bond between two Lewis-acidic sites in **I** and **III**, each bearing good leaving groups, presents both challenges and opportunities: on the one hand, this unique combination promotes spontaneous disproportionation and vigorous decomposition upon exposure to air and moisture.[7–10] On the other hand, it enables uncatalyzed diboration reactions using **I**,[11–17] the *in situ* generation of versatile $[SiX_3]^-$ nucleophiles from **III** upon simple halide addition,[18,19] and extensive late-stage derivatization at the B–X and Si–X bonds of the primary products. Thus, in contrast to the abundant bis(pinacolato)diboron (pinB–Bpin), whose B atoms are electronically tamed by $O=B$ π-donation and serve primarily as transmetallation

partners in Suzuki–Miyaura cross-couplings,[20–22] type-**I** halogenoboranes are tailored for applications where the B atoms are to remain as property-determining functional units in the final molecule.[23–29] Likewise, the Si_2X_6/X^- trichlorosilylation system and the controlled disproportionation of Si_2X_6 with NR_3 (ref. 30–32) have proven valuable for the synthesis of extensively derivatizable organosilanes,[33–36] oligotetrelanes,[37–42] and silicon clusters.[43–50] In contrast to **I**, **III** undergoes no spontaneous 1,2-additions to unsaturated organic substrates, and theoretical studies predict a prohibitively high activation barrier without a catalyst.[51,52]

Given the indispensable role of borylated[53,54] and silylated[55] building blocks in synthesis, it is desirable to combine both types of functional groups within a single building block, for which silylboranes of the type $R_2B–SiR_3$ are the most obvious candidates.[56–60] Electronically stabilized representatives such as the prominent pinB–SiMe₂Ph typically require activation by (precious) metal complexes prior to addition across $C=C$ double[61–63] or $C≡C$ triple bonds.[64–72] In only a few cases, the addition of a (Lewis) base (KO*t*Bu,[73,74] $KN(SiMe_3)_2$,[75] PR_3,[76] pyridines[77,78]) has been sufficient to replace the transition metal catalyst in silaboration reactions. Yet, a significant proportion of base-catalyzed silylborane transformations results in incorporation of either the boryl[74,79–84] or the silyl[85–91] group,[92] while the respective counterpart is discarded. So far, a single

[a]Institut für Anorganische und Analytische Chemie, Goethe-Universität Frankfurt, Max-von-Laue-Straße 7, D-60438 Frankfurt am Main, Germany. E-mail: matthias. wagner@chemie.uni-frankfurt.de

[b]School of Chemistry and Forensic Science, University of Kent, Park Wood Rd, Canterbury CT2 7NH, UK
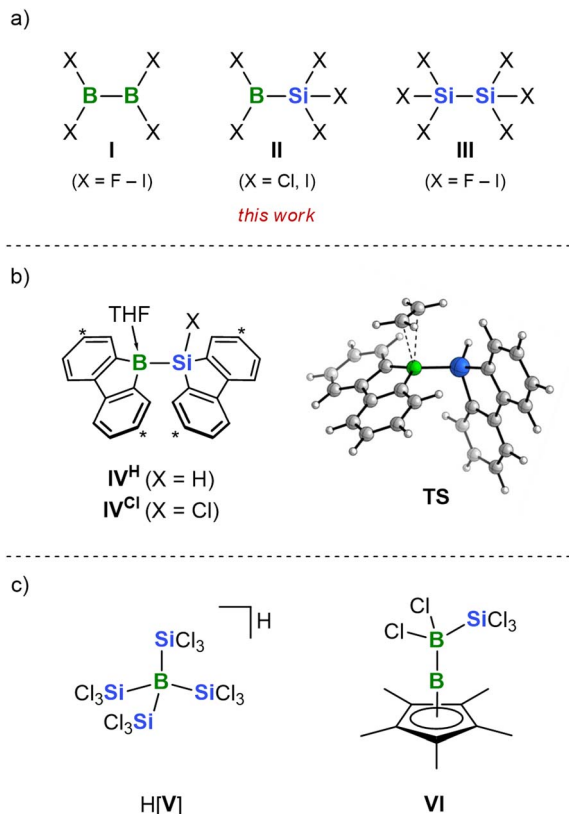
† These authors contributed equally to this work.

Fig. 1 (a) Perhalogenated diboranes(4) (**I**), disilanes (**III**), and the perhalogenated silylboranes (**II**) studied in this work. (b) Previously studied silylboranes (**IV**) capable of undergoing uncatalyzed silaboration reactions (C atoms marked with asterisks bear *t*Bu substituents); computed transition state (**TS**) for the silaboration of ethylene with **IV**^{H} (*t*Bu groups have been omitted in the calculations). (c) Silylborates H[**V**] and **VI** bearing some structural similarity with **II**.

uncatalyzed silaboration reaction has been reported, employing compounds **IV**^{H} and **IV**^{Cl} in THF (Fig. 1b).[93,94] Key to this transformation is the incorporation of both the B and Si atoms of **IV** into planar heterofluorene scaffolds, which—compared to pinB–SiMe$_2$Ph—enhances their exposure to the unsaturated substrate while reducing π-electron donation into the vacant B(p$_z$) orbital (quantum-chemical calculations exclude a promoting effect of the THF ligand on B–Si-bond cleavage; *cf.* the transition state **TS** of olefin silaboration shown in Fig. 1b). Based on this background and the high reactivity of **I** and **III**, we reasoned that the perhalogenated silylborane **II** (Fig. 1a) as a silaboration reagent should uniquely combine a strong tendency towards B–Si heterolysis and diverse opportunities for subsequent derivatization. Herein, we demonstrate that type-**II** compounds with X = Cl, I can indeed be readily synthesized on a multigram scale. We provide a full characterization of their B-adducts with various Lewis bases and show that the Cl derivative Cl$_2$B–SiCl$_3$ can even be isolated in its free form as a distillable liquid. Notably, we disclose that both uncatalyzed 1,2- and rare 1,1-addition reactions to alkenes have been achieved. Only a few previously reported compounds share structural or electronic features with **II**. Among them are the borate H[**V**] and

the *nido* cluster **VI** (Fig. 1c).[95,96] Furthermore, the molecular structure of the anion [Cl$_3$B–SiCl$_3$]$^-$ has been determined through single crystal X-ray structure analysis of the salt [(TMS$_2$N)SiCl$_2$–B(η^5-C$_5$Me$_5$)][Cl$_3$B–SiCl$_3$] (TMS = Me$_3$Si).[97]

Results and discussion

The synthesis of B$_2$X$_4$ (**I**) dates back to 1925, but for decades remained the domain of specialists capable of mastering the technically challenging gas-phase protocols of the time.[98–100] A major breakthrough came in 1981, when Nöth *et al.* obtained B$_2$Br$_4$ in good yields by converting B$_2$(OMe)$_4$ with BBr$_3$ through a convenient solution-phase synthesis.[101] In 2017, Braunschweig *et al.* extended this approach to the other perhalogenated diboranes(4) *via* solution-phase reactions of B$_2$Br$_4$ with SbF$_3$, GaCl$_3$, and BI$_3$.[5]
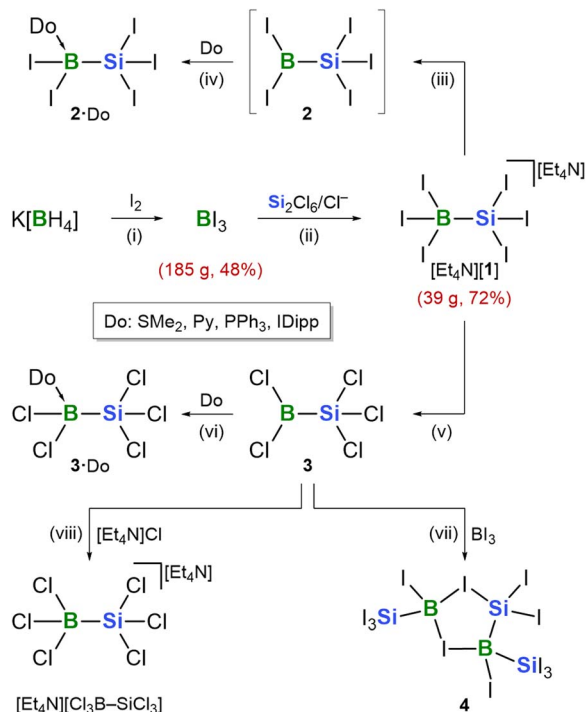
Si$_2$Cl$_6$, a side product of several large-scale processes in the silicon industry,[102] is commercially available; quantitative Cl/F exchange with SbF$_3$ affords Si$_2$F$_6$.[103] The perbromo- and periododisilanes are accessible from Si$_2$Ph$_6$ by Ph/X exchange with MeC(O)X/AlX$_3$ (X = Br, I).[104]

Analogous to how B$_2$Br$_4$ and Si$_2$Cl$_6$ grant access to their respective compound classes, the salt [Et$_4$N][I$_3$B–SiI$_3$] ([Et$_4$N][**1**]; Scheme 1) serves as a key starting material for developing perhalogenated silylboranes. Several years ago, we first reported [Et$_4$N][**1**], primarily to demonstrate the *in situ* formation of [SiCl$_3$]$^-$ as the reactive intermediate in the Si$_2$Cl$_6$/Cl$^-$ trichlorosilylation system *via* Lewis-adduct formation with BX$_3$.[19] Our study revealed that (excess) BI$_3$ is a more effective trapping reagent than BCl$_3$, because it is the stronger Lewis acid and outcompetes coexisting Si$_2$Cl$_6$ for coordination with [SiCl$_3$]$^-$, thus suppressing the formation of unwanted oligosilane side products.[18] By thoroughly optimizing the original protocol, the yield of [Et$_4$N][**1**] was increased from ≈45% to ≈70%, and the synthesis was scaled to ≈40 g (Scheme 1). A key improvement is the addition of a second portion of BI$_3$ (0.1 eq.) toward the end of the reaction, following the initial addition of 2 eq. BI$_3$. This prevents contamination of [Et$_4$N][**1**] with [Et$_4$N][I$_2$ClB–SiI$_3$], previously described as an 'unknown side product'; its identity has now been unequivocally confirmed by X-ray crystallography (Fig. S102). This finding laid the foundation for a systematic exploration of perhalogenated silylboranes.

Syntheses of new compounds

The quantitative Si–Cl/Si–I exchange during the formation of [Et$_4$N][**1**] is advantageous, as iodinated products crystallize more readily in pure form than their chlorinated congeners. However, in combination with the salt-like nature of [Et$_4$N][**1**], this results in extremely low solubility, posing challenges for subsequent transformations. As initial derivatizations, we consequently replaced one I$^-$ ligand in [Et$_4$N][**1**] with neutral donor ligands (Do) bearing solubilizing substituents. To this end, suspensions of [Et$_4$N][**1**] and Krossing's salt (Li[Al(OC(CF$_3$)$_3$)$_4$])[105] in CH$_2$Cl$_2$ were treated with the respective ligand at rt [Do: SMe$_2$, pyridine (Py), PPh$_3$, 1,3-bis(2,6-diisopropylphenyl)-1,3-dihydro-2*H*-imidazol-2-ylidene (IDipp);

Scheme 1 Optimized synthesis of [Et₄N][**1**], enabling multigram-scale access to this key starting material. Conversion of the poorly soluble salt [Et₄N][**1**] into moderately soluble neutral donor adducts **2**·Do (Py: pyridine; IDipp: 1,3-bis(2,6-diisopropylphenyl)-1,3-dihydro-2*H*-imidazol-2-ylidene). Formation of the liquid perchlorinated silylborane **3** and its adducts **3**·Do. Reaction of **3** with BI₃ does not furnish **2**, but yields the five-membered ring compound **4**, characterized by X-ray crystallography. Reagents and conditions: (i) 1.25 eq. I₂, *n*-heptane, 80 °C, min. 10 h, 48% yield; (ii) 1 eq. [Et₄N]Cl, 0.5 eq. Si₂Cl₆, 0.05 eq. BI₃, CH₂Cl₂, rt, 24 h, 72% yield; (iii) 1.1 eq. Li[Al(OC(CF₃)₃)₄], *o*DFB, rt, 24 h; (iv) 1.1 eq. Do: SMe₂, Py, PPh₃, IDipp, CH₂Cl₂, rt, 24 h, SMe₂ = 91%, Py = 83%, PPh₃ = 87%, IDipp = 71% yield; (v) *Method A*: 2.1 eq. GaCl₃, 80 °C, 1 h, 96% yield; *Method B*: 2.1 eq. GaCl₃, *o*DFB, rt, 15 min; (vi) 1.0 eq. Do: SMe₂, Py, PPh₃, IDipp, *o*DFB, rt, 15 min, SMe₂ = 94%, Py = 95%, PPh₃ = 91%, IDipp = 89% yield; (vii) 2 eq. BI₃, *o*DFB, rt, 15 min, 95% yield; (viii) 1 eq. [Et₄N]Cl, *o*DFB, rt, 15 min, 92% yield.

Scheme 1]. After filtration, colorless crystals of the corresponding adducts **2**·Do readily grew from the filtrate (yields: SMe₂ = 91%; Py = 83%; PPh₃ = 87%; IDipp = 71%). In stark contrast to BI₃, which is sensitive to sunlight, **2**·Do exhibit remarkable photostability, with no signs of decomposition upon light exposure.

Cation-exchange using Krossing's salt precipitated LiI as an insoluble byproduct instead of releasing soluble [Et₄N]I, thereby driving the quantitative I⁻/Do substitution and facilitating the isolation of pure **2**·Do. Most of the second byproduct, [Et₄N][Al(OC(CF₃)₃)₄], remained in the mother liquor; residual traces adhering to the crystals of **2**·Do were removed by rinsing with *ortho*-difluorobenzene (*o*DFB). To characterize the primary [Et₄N]⁺/Li⁺ cation-exchange product, an equimolar mixture of [Et₄N][**1**] and Li[Al(OC(CF₃)₃)₄] was stirred in *o*DFB. The resulting solid, which proved insoluble in all common inert solvents, was analyzed by solid-state ¹¹B and ²⁹Si NMR spectroscopy. The data indicated the presence of Li[**1**] along with free **2** (and

already eliminated LiI; see the SI for more details). Given that the insolubility of the free silylborane I₂B–SiI₃ (**2**) precluded its isolation and characterization in pure form, we next turned our attention to the synthesis of its perchlorinated congener Cl₂B–SiCl₃ (**3**; Scheme 1).

The targeted full I/Cl substitution was straightforwardly achieved by stirring [Et₄N][**1**] with 2 eq. GaCl₃—either as a solid mixture that gradually liquefied upon intermittent heating to 80 °C (*Method A*), or in *o*DFB (*Method B*). Neat **3** (*Method A*) or its calibrated *o*DFB solution (*Method B*) was obtained by gas-phase transfer of all volatiles under static vacuum at rt into a glass vessel cooled with liquid N₂.[106] The colorless donor adducts **3**·Do were harvested in crystalline form after stirring **3** and Do in *o*DFB for 15 min at rt (Scheme 1; yields: SMe₂ = 94%; Py = 95%; PPh₃ = 91%; IDipp = 89%).

As noted above, the perchlorinated analogue [Et₄N][Cl₃B–SiCl₃] of [Et₄N][**1**] is not accessible through trapping of *in situ*-generated [SiCl₃]⁻ with BCl₃. With the free silylborane **3** in hand, we have now demonstrated that its reaction with [Et₄N]Cl in *o*DFB affords [Et₄N][Cl₃B–SiCl₃] in >90% yield (Scheme 1). This confirms that the BCl₃-based trapping experiment has failed not due to an inherent instability of [Cl₃B–SiCl₃]⁻, but rather because of interfering side reactions that dominate in the mixture BCl₃/Si₂Cl₆/[Et₄N]Cl.

As a final approach, we attempted to access pure **2** *via* Cl/I exchange at **3** using 2 eq. BI₃ in *o*DFB. Instead of the target compound, we obtained the five-membered ring species **4** in good yields (Scheme 1). Its solid-state structure provides valuable insight to rationalize fundamental reactivity patterns of perhalogenated silylboranes (see below).

NMR-spectroscopic, mass-spectrometric, and X-ray-crystallographic characterization of new compounds[107]

Liquid-phase NMR spectra were recorded at rt in CD₂Cl₂ and on a sample of neat **3**.

The free perchlorinated silylborane **3** gives rise to a singlet at 63.7 ppm in the ¹¹B NMR spectrum and to a 1 : 1 : 1 : 1 quartet at −8.2 ppm in the ²⁹Si NMR spectrum (¹*J*(B,Si) ≈ 200 Hz; Fig. S24, S25).

Tetracoordinate species typically show ¹¹B NMR signals in the high-field region of the spectrum. The specific chemical shift values are governed by two main factors: (i) the electron density at the ¹¹B nucleus, which reflects the donor strength of the coordinating ligand, and (ii) shielding effects arising from the magnetic anisotropy of the electron shells of the donor atoms, which are especially pronounced for heavier donors.[108] To sidestep a comparative evaluation of magnetic anisotropy effects, we restrict our analysis to **2**·Py *vs.* **2**·IDipp (2nd-row donor atoms; δ(¹¹B) = −24.8 *vs.* −37.1) and **2**·SMe₂ *vs.* **2**·PPh₃ (3rd-row donor atoms; δ(¹¹B) = −31.8 *vs.* −40.6). The observed trends align with the expectation that the more stable adducts are formed with IDipp and PPh₃, respectively. The chlorinated compounds **3**·Py *vs.* **3**·IDipp (δ(¹¹B) = 3.7 *vs.* −4.4) and **3**·SMe₂ *vs.* **3**·PPh₃ (δ(¹¹B) = 1.4 *vs.* −3.4) exhibit the same chemical-shift trends within each pair as observed for the corresponding **2**·Do adducts. However, all four signals appear at markedly lower field, which we attribute to decreased magnetic anisotropy

shielding when going from the $BI_2(Do)$ to the $BCl_2(Do)$ fragments. The ^{29}Si NMR resonances of **2·Do** and **3·Do** were not detectable in the solution spectra, owing to unresolved $^1J(B,Si)$ coupling and broadening induced by the quadrupolar ^{11}B nucleus ($S = 3/2$).[108] The ^{31}P NMR spectra of **2·PPh₃** and **3·PPh₃** are characterized by multiplet resonances at -7.2 and 2.1 ppm, respectively.

Electron ionization (EI) mass spectra were recorded for the full series of donor adducts **2·Do** and **3·Do** (introduced as solids). In most cases, we observed the molecular ion peak $[(Do)X_2B–SiX_3]^{•+}$ and/or the peak corresponding to the donor-free silylborane $[X_2B–SiX_3]^{•+}$, typically with low intensity ($X = Cl, I$; see the SI for details). Most adducts appear to release their neutral Do ligand under the measurement conditions—except for IDipp, which resists elimination. Prominent fragmentation products included $[(Do)BSiX_4]^+/[BSiX_4]^+$ and $[(Do)BX_2]^+$. The latter may arise either by $[SiX_3]^•$ loss from the parent ion or via a concerted pathway: $[SiX_2]$ extrusion from $[(Do)X_2B–SiX_3]^{•+}$, followed by $X^•$ elimination from the resulting $[(Do)BX_3]^{•+}$ intermediate. This, in turn, raises the question—relevant for later reactivity studies—of whether neutral **2·Do** and **3·Do** might undergo thermal $[SiX_2]$ extrusion. To probe this, **2·IDipp** was heated with the silylene-trapping reagent 2,3-dimethyl-1,3-butadiene (DMB; 10 eq.) in oDFB at 100 °C for 10 days in a flame-sealed NMR tube. $[SiI_2]$ was subsequently identified by GC-MS as its cycloadduct, 1,1-diiodo-3,4-dimethyl-1-silacyclopent-3-ene (Fig. S2).[109] Consistently, the reaction mixture showed an ^{11}B NMR signal corresponding to the byproduct BI_3·IDipp formed through reductive elimination at the Si(IV) center of **2·IDipp** (-77.3 ppm; confirmed by comparison with an authentic sample and X-ray crystal structure analysis of a single crystal grown in the NMR tube).

All eight adducts **2·Do** and **3·Do** were structurally characterized by X-ray crystallography (Fig. S103–S106 and S109–S112).[110] Given the particular relevance of **2·SMe₂** to silaboration reactions (see below), the molecular structures of this compound and its perchlorinated congener **3·SMe₂** are shown as representative examples in Fig. 2a. All B–Si-bond lengths in **2·Do/3·Do** fall within a narrow range of 2.005(3) to 2.043(4) Å, indicating that this parameter is not significantly influenced by either the nature of Do or the halogen ligand. In contrast, the B–Do bond lengths and the degree of pyramidalization at the B atom in the X_2BSi fragments support the a priori expectations that (i) SMe₂ is the weakest among the four donors Do, and (ii) the iodinated compound **2** is more Lewis acidic than its chlorinated analogue **3**.[111]

Each molecule of **4** contains two chiral B atoms, giving rise to four possible diastereomers (Fig. 2b, left). In the lattice of the examined single crystal, two diastereomers [(S,S)/(S,R)] occupy the same crystallographic site in a 73 : 27 ratio, which leads to partial disorder involving the B(2)–Si(3) unit. This disorder, together with the comparatively weak scattering contribution of the light B atoms relative to the multiple heavy I atoms, limits the precision with which the B-atom positions and associated structural parameters can be determined. The five-membered ring in **4** features bridging I atoms (B–μ(I)–B and B–μ(I)–Si), resulting in tetracoordinate rather than tricoordinate, electron-
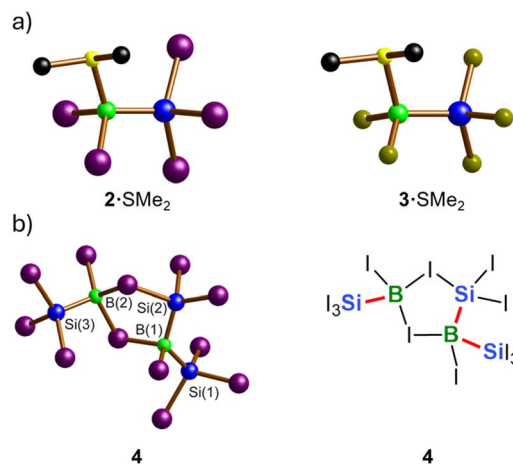

Fig. 2 (a) Solid-state structures of **2·SMe₂** (β-polymorph; left) and **3·SMe₂** (right); (b) solid-state structure of the (S,S)-diastereomer of **4** (left) and its corresponding structural formula, with one BSi and one BSi₂ moiety highlighted in red (right). H atoms are omitted for clarity. Color code: B: green, C: black, Si: blue, S: yellow, Cl: yellow-green, I: violet.

deficient B sites (Fig. 2b, left).[112] This feature prompts speculation that the extremely insoluble species **2** may adopt a polymeric or dimeric structure in the solid state, possibly featuring B_2I_2Si five-membered rings, with a single I atom replacing the Si(1)I₃ substituent. Moreover, the presence of both a BSi and a BSi₂ moiety in **4** (indicated by red-colored bonds in Fig. 2b, right) suggests that our methodology may provide access not only to perhalogenated silylboranes but also to disilylboranes.

Silaboration reactions with 2·Do and 3·Do

One of the primary motivations for developing **2·Do** and **3·Do** was to create highly reactive silaboration reagents that allow for the simultaneous introduction of both derivatizable functional groups, ideally under catalyst-free conditions. Ethylene was selected as the initial model substrate for two main reasons: (i) its gaseous nature and lack of activating substituents make its silaboration particularly challenging, and (ii) the expected products are highly symmetric molecules with low molecular

Table 1 Conditions and product distributions for the reactions of the adducts **2·Do** or **3·Do** with an excess of ethylene in sealed NMR tubes

Adduct	Conditions	Product(s)
2·SMe₂	CD₂Cl₂, 6 d, 80 °C	5·SMe₂, 98%
2·SMe₂/0.1 BI₃	**CD₂Cl₂, 12 h, rt**	**5·SMe₂, 85%**
2·Py	oDFB, 20 d, 120 °C	5·Py, 97%
2·PPh₃	oDFB, 20 d, 120 °C	5·PPh₃, BI₃·PPh₃[b]
2·IDipp	oDFB, 6 d, 100 °C	BI₃·IDipp[b]
3·SMe₂	CD₂Cl₂, 31 d, 80 °C	6·SMe₂, BCl₃·SMe₂[b]
3·Py	oDFB, 7 d[a], 120 °C[a]	BCl₃·Py[b]
3·PPh₃	oDFB, 17 d, 120 °C	BCl₃·PPh₃[b]
3·IDipp	oDFB, 7 d[a], 120 °C[a]	BCl₃·IDipp[b]

[a] After the initial heating period, heating was continued at 140 °C for 1 day and at 160 °C for 1 day. [b] The reaction mixture contained unconsumed starting material.

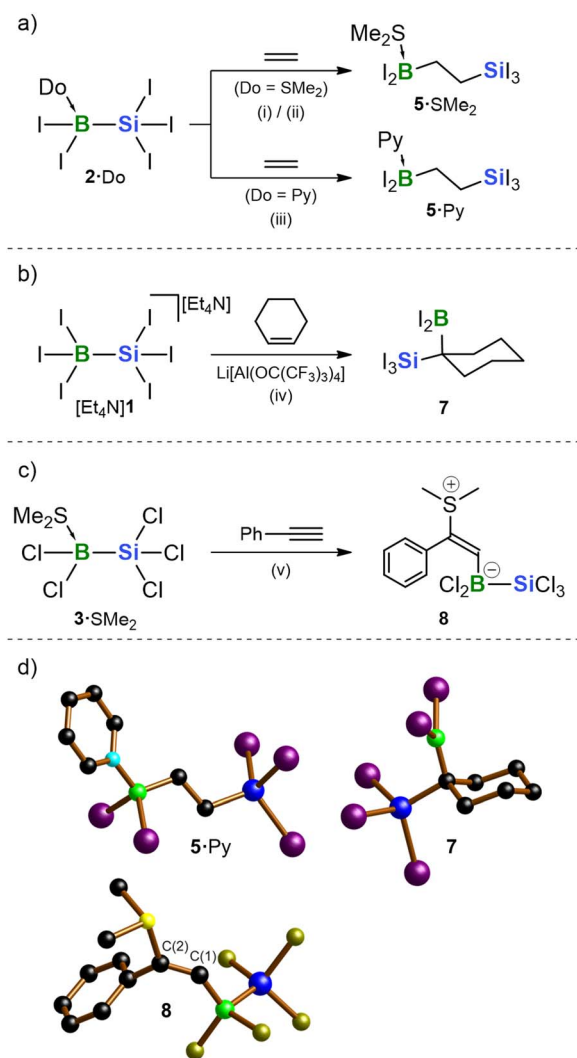weight, which facilitates analysis by NMR spectroscopy and mass spectrometry.[61,94]

The reactions were carried out by heating an excess of ethylene with $2 \cdot Do$ or $3 \cdot Do$ in CD_2Cl_2 or oDFB in sealed NMR tubes (Table 1 and Scheme 2a). oDFB was used when high temperatures and/or prolonged reaction times posed a risk of I/Cl exchange with CD_2Cl_2; for NMR measurements, oDFB was replaced with CD_2Cl_2 prior to measurement.

To evaluate general reactivity trends, we employed the pure silylborane adducts without added promoters. Under these conditions, $2 \cdot SMe_2$ underwent quantitative conversion with

ethylene to afford the 1,2-silaboration product $Me_2S \cdot I_2B-C_2H_4-SiI_3$ ($5 \cdot SMe_2$; Table 1 and Scheme 2a). This transformation proceeded to completion at 80 °C within 6 days. Likewise, $2 \cdot Py$ gave similarly high yields, albeit under even harsher conditions (120 °C, 20 d). At similar temperatures and reaction times, $2 \cdot PPh_3$ was only partially consumed; the fraction that reacted generated both the silaboration product $5 \cdot PPh_3$ and the thermolysis product $BI_3 \cdot PPh_3$. Among the perchlorinated analogues, only $3 \cdot SMe_2$ produced a notable amount of the corresponding 1,2-silaboration product. However, this transformation took five times longer than the reaction of $2 \cdot SMe_2$ and furnished $Me_2S \cdot Cl_2B-C_2H_4-SiCl_3$ ($6 \cdot SMe_2$; Table 1) contaminated with residual starting material and the side product $BCl_3 \cdot SMe_2$. No silaboration was observed for the other adducts $2 \cdot Do$ and $3 \cdot Do$; instead, they formed varying amounts of $BX_3 \cdot Do$, likely due to thermally induced $[SiX_2]$ extrusion, as discussed above and corroborated by our previous trapping experiments with DMB. To promote the reaction between $2 \cdot SMe_2$ and ethylene, BI_3 (0.1 eq.) was added to the mixture. Now, silaboration proceeded smoothly at rt within 12 h, affording $5 \cdot SMe_2$ in high yields (85%; entry 2 in Table 1). This final result of our systematic screening thus offers a practical and efficient access route to this promising functionalized building block. Notably, neither the $Li[1]/2/LiI$ mixture nor free 3 provided further improvement, as both led to pronounced side reactions, presumably including ethylene polymerization. We further emphasize that haloboration did not compete with silaboration under any of the tested conditions.

Based on these experimental findings, two key principles emerge to guide further synthetic applications: (i) the highly reactive free species 2 and 3 must be tamed by adduct formation with a suitable donor to prevent non-selective transformations. In this regard, the soft ligand SMe_2 performs best in terms of product selectivity while still allowing for reasonable temperatures and reaction times—especially when 0.1 eq. of BI_3 is added as a promoter, which likely generates small concentrations of the free Lewis acid 2 in situ. (ii) The iodinated adducts are more effective in silaborations than their chlorinated congeners. From that, we offer the following mechanistic interpretations: (i) silaborations with $2 \cdot Do$ and $3 \cdot Do$ are apparently not initiated by donor-induced B–Si-bond cleavage. Instead, displacement of Do by π-bonded ethylene must precede the 1,2-addition step (comparable B$\cdots$olefin complexes have been structurally characterized by Yamaguchi et al.[113]). (ii) To maximize the interaction between the vacant $B(p_z)$ orbital and the π-electron cloud of ethylene, competing π-backbonding from X to B must be minimized, which accounts for the superior suitability of X = I (2-type compounds) over Cl (3-type compounds). A comprehensive quantum-chemical assessment of the overall reaction mechanism is provided below.

In a second reactivity test, a mixture of $2 \cdot SMe_2$ and the internal olefin cyclohexene in oDFB was heated to 120 °C for 24 days. Subsequent ^{11}B NMR analysis of the sample showed essentially one signal at -11.6 ppm, indicating quantitative and selective conversion. As such forcing reaction conditions lack practical relevance, efforts were directed toward significantly accelerating the reaction prior to detailed product analysis.

Scheme 2 (a) 1,2-Silaborations of ethylene with $2 \cdot SMe_2$ or $2 \cdot Py$ afford $5 \cdot SMe_2$ or $5 \cdot Py$. (b) 1,1-Silaboration of cyclohexene with $[Et_4N]1/Li[Al(OC(CF_3)_3)_4]$ furnishes 7. (c) Reaction of phenylacetylene with $3 \cdot SMe_2$ leads to the addition of the $3/SMe_2$ Lewis pair across the C≡C bond to give 8. (d) Solid-state structures of $5 \cdot Py$, 7, and 8; H atoms are omitted for clarity. Color code: B: green, C: black, N: pale blue, Si: blue, S: yellow, Cl: yellow-green; I: violet. Reagents and conditions: (i) exc. ethylene, CD_2Cl_2, 80 °C, 6 d, 98% yield; (ii) exc. ethylene, 0.1 eq. BI_3, CD_2Cl_2, rt, 12 h, 85% yield; (iii) exc. ethylene, oDFB, 120 °C, 20 d, 97% yield; (iv) 10 eq. cyclohexene, 1 eq. $Li[Al(OC(CF_3)_3)_4]$, oDFB, rt, 15 min, 99% yield; (v) 5 eq. phenylacetylene, CH_2Cl_2, rt, 1 d, 37% yield.

In this instance, the addition of BI_3 as a promoter did not prove beneficial. However, a successful outcome was ultimately achieved using an equimolar mixture of $[Et_4N][1]$ and $Li[Al(OC(CF_3)_3)_4]$ in oDFB, which effected complete conversion within only 15 min at rt. It is evident that the increased kinetic protection of the C=C double bond in this case suppresses unwanted side reactions, even in the absence of any donor ligand apart from the residual I^- ions. More remarkably, olefin internalization exerts a decisive effect on regioselectivity: the reaction with cyclohexene selectively afforded the 1,1-silaboration product **7** rather than the 1,2-isomer (Scheme 2).[114] Such a transformation is unprecedented—not only in silaboration but also in the related diboration or disilylation of olefins.[115]

In a final test experiment, phenylacetylene was chosen as the third representative substrate. Since the iodinated $2 \cdot SMe_2$ led to complex product mixtures, we turned to the chlorinated analogue $3 \cdot SMe_2$, which underwent complete conversion at rt after 1 day. From the reaction mixture, the zwitterionic species **8** crystallized in 37% yield (Scheme 2). Unlike $5 \cdot Do$ and **7** (Do = SMe_2, Py), **8** is not generated via silaboration but instead represents the typical outcome of a concerted reaction between a free thioether Lewis base and a free borane Lewis acid acting on the same C≡C triple bond.[116–122] This finding thus supports our earlier assumption that replacement of the B-bonded donor Do with the unsaturated substrate constitutes the initial step in the reactions of $2 \cdot Do$ and $3 \cdot Do$. In the case of olefin substrates, both a boryl and a silyl group are introduced into the molecule. Yet, with phenylacetylene, the B–Si bond remains intact, and SMe_2 is instead transferred to the substrate. In **8**, the B atom is attached to the terminal position of the resulting olefin, while the SMe_2 substituent resides near the phenyl ring. This can be explained by the fact that the positive charge accumulated on the carbon framework during electrophilic borylation is better stabilized by resonance at the α-position relative to the phenyl ring.

NMR-spectroscopic and X-ray crystallographic characterization of $5 \cdot Do$, 7, and 8 (ref. 107)

The ^{11}B NMR spectra of the 1,2-silaboration products, $5 \cdot SMe_2$ and $5 \cdot Py$, exhibit resonances at -18.9 and -14.0 ppm, respectively, consistent with the presence of tetracoordinate B nuclei.[108] In contrast, the ^{11}B NMR signal of the 1,1-silaboration product **7** appears at 53.5 ppm, indicative of a tricoordinate B center.[108] The ^{29}Si NMR shifts of $5 \cdot SMe_2$, $5 \cdot Py$, and **7** are very similar with values of -115.1, -114.8, and -122.8 ppm, respectively. Furthermore, all three compounds give rise to signals exclusively in the aliphatic region of their ^{1}H NMR spectra, confirming complete consumption of the C=C double bonds present in the starting materials. The resonances of the axial and equatorial H atoms within the cyclohexyl moiety of compound **7** are distinctly resolved, indicating that bulky substituents on the saturated ring act as effective conformational locks on the NMR timescale.[123,124] The ^{11}B NMR spectrum of **8** is characterized by a resonance at -2.6 ppm. As in the cases of $2 \cdot Do$ and $3 \cdot Do$, the ^{29}Si NMR signal of the B-bonded Si atom is broadened beyond detection. A singlet at $\delta(^1H) = 7.35$,

together with a corresponding broad resonance at $\delta(^{13}C) = 163.1$, is consistent with the presence of an olefinic fragment in **8**.

The molecular structures of $5 \cdot SMe_2$ (Fig. S115), $5 \cdot Py$, and **7** (Scheme 2d), confirm their proposed identities as 1,2- and 1,1-silaboration products, respectively. The C–C-bond length in $5 \cdot Py$ falls within the typical single-bond range (1.533(4) Å), as do all C–C bonds in **7**. As expected,[123,124] the bulkier SiI_3 substituent occupies an equatorial position, whereas the less bulky BI_2 group adopts an axial orientation in the cyclohexane ring of **7**. In contrast to compound **4** (Fig. 2), there is no B–μ(I)–Si bridge in **7**; rather, the boryl group remains trigonal-planar coordinated. Nonetheless, the vacant $B(p_z)$ orbital may acquire some electron density from the occupied Si–C σ orbital, reminiscent of the well-known stabilization of carbenium ions bearing β-positioned silyl groups (see below).[125] The C(1)–C(2) distance in compound **8** is 1.335(5) Å, characteristic of a double bond (Scheme 2d). The S and B atoms adopt a mutual E configuration, with the sterically demanding (silyl)boryl substituent located at the terminal position of the styrene core.

Quantum-chemical calculations rationalizing the 1,2- $vs.$ 1,1-silaboration of ethylene $vs.$ cyclohexene to give $5 \cdot SMe_2$ $vs.$ 7

For the reactions of $2 \cdot SMe_2$ and $[Et_4N][1]/Li[Al(OC(CF_3)_3)_4]$ with the olefins, two scenarios were examined: 1,2-silaboration and 1,1-silaboration. Potentially competing haloboration pathways[126] as well as, for $2 \cdot SMe_2$, the hypothetical addition of the $Me_2S/I_2B–SiI_3$ Lewis pair to ethylene, were also considered but found to be irrelevant (see the SI for corresponding reaction pathways, activation barriers, and reaction energies). Fig. 3 shows the plausible silaboration sequences for ethylene (a) and cyclohexene (b). As a first important result, the experimentally observed products correspond to pathways that are both kinetically and thermodynamically favored (highlighted in red).

In the reaction of $2 \cdot SMe_2$ with ethylene, the SMe_2 donor must first dissociate to generate a vacant coordination site at the B atom for olefin binding. The dissociation requires an energy input of 14.6 kcal mol^{-1} ($cf.$ Fig. S134). However, the presence of BI_3 renders the in $situ$ release of the active silaboration reagent **2** significantly less endergonic ($2 \cdot SMe_2 + BI_3 \rightarrow 2 + BI_3 \cdot SMe_2$; $\Delta G = 4.8$ kcal mol^{-1}). Subsequent ethylene binding to free **2** is endergonic by an additional 5.4 kcal mol^{-1}. The resulting intermediate, $2 \cdot (C_2H_4)$, features a strongly pyramidalized B atom $[\sum(I–B–I/Si) = 320.2°]$; the ethylene ligand remains essentially planar.[127] The reaction proceeds via transition state **TS1**, characterized by B–Si-bond cleavage and the concerted formation of a C–Si bond. The 1,2-silaboration product **5** lies -21.7 kcal mol^{-1} below the starting materials, with an overall activation barrier of only 15.7 kcal mol^{-1}. In the final step, **5** acquires an SMe_2 ligand from $2 \cdot SMe_2$ to afford $5 \cdot SMe_2$ and free **2** with a similar endoergicity as observed in the case of $2 \cdot SMe_2/BI_3$, explaining why only minor amounts of BI_3 are necessary to promote the silaboration at rt. The alternative 1,1-silaboration of ethylene to furnish **12** would have to proceed via the much higher–energy transition state **TS2** ($\Delta G^{\ddagger} =$
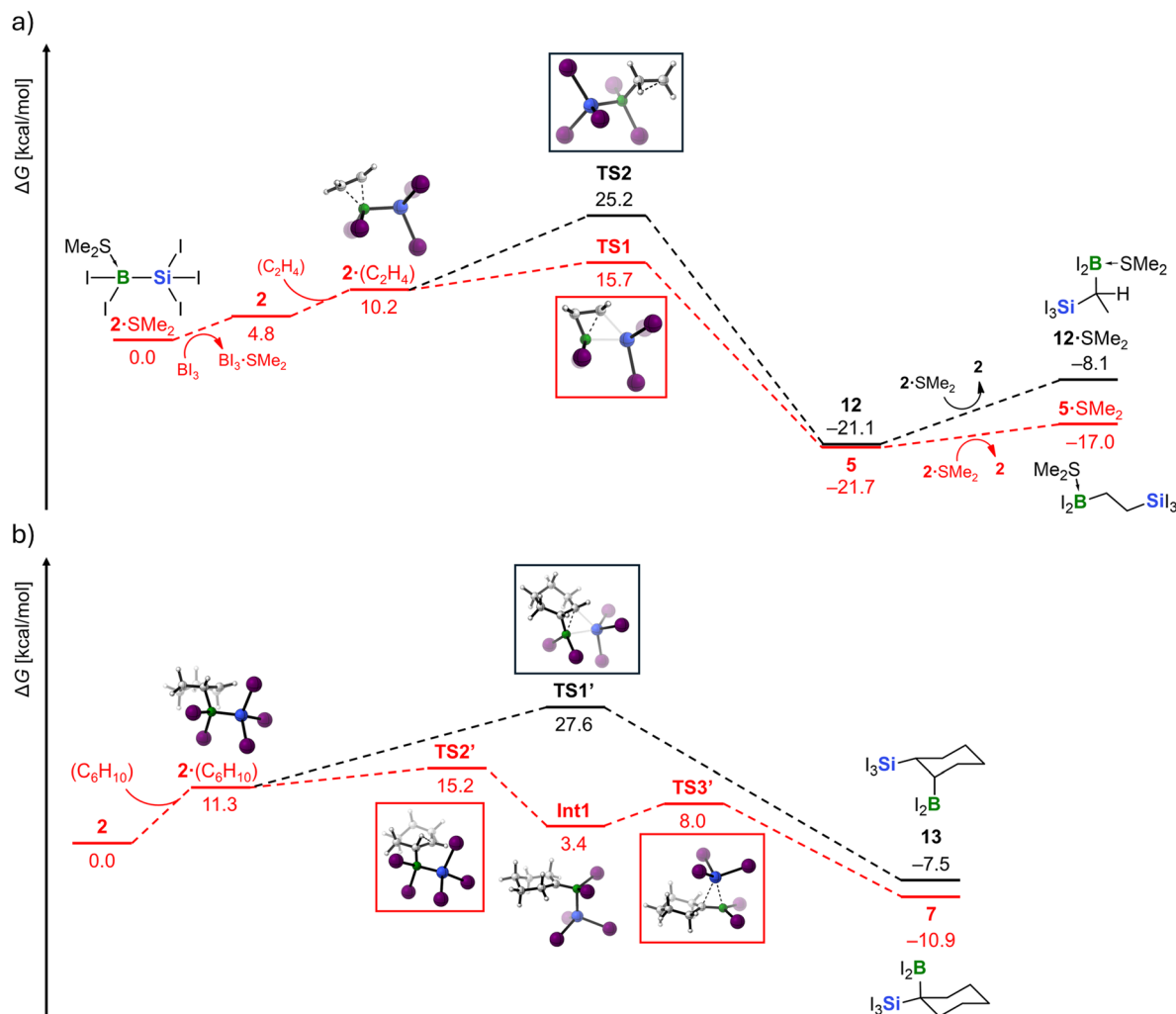
Fig. 3 Computed reaction mechanisms for (a) the observed 1,2-silaboration of ethylene with $2 \cdot SMe_2/0.1\ BI_3$ (red) *vs.* the not observed 1,1-silaboration pathway (black) and (b) the observed 1,1-silaboration of cyclohexene with **2** (red) *vs.* the not observed 1,2-silaboration pathway (black). Color code: H: white, B: green, C: grey, Si: blue, I: violet. The Gibbs free energy changes (ΔG) were computed at the SMD(DCM)/PBE0-D3(BJ)/def2-QZVPPD level of theory, using geometries optimized at the SMD(DCM)/PBE0-D3(BJ)/def2-SVPD level. Note: compounds **9–11** appear in the SI as part of theoretically examined but energetically unfavorable alternative mechanisms.

25.2 kcal mol^{-1} relative to the starting materials) and is thus not observed.

Due to the modified protocol used for the silaboration of cyclohexene, dissociation of SMe$_2$ is not an issue here. Instead, free **2** can directly interact with the added olefin. Formation of the primary olefin complex $2 \cdot (C_6H_{10})$ is somewhat more endergonic than in the case of ethylene ($\Delta G = 11.3$ *vs.* 5.4 kcal mol^{-1}), which can be attributed partly to steric factors and partly to a more pronounced reorganization energy: while the B atom in $2 \cdot (C_6H_{10})$ is comparably pyramidalized as in $2 \cdot (C_2H_4)$, one B-bonded C atom now also deviates significantly from planarity [$\sum(C-C-C/H) = 348.2°$].[127] Starting from $2 \cdot (C_6H_{10})$, two subsequent transition states are most relevant: **TS1′** leads, *via* an overall activation barrier of 27.6 kcal mol^{-1}, to the (experimentally unobserved) syn-1,2-silaboration product **13** ($\Delta G = -7.5$ kcal mol^{-1}). In contrast, **TS2′**, which lies 12.4 kcal mol^{-1} lower in energy than **TS1′**, corresponds to a 1,2-

hydride shift leading to intermediate **Int1**. Subsequent 1,2-silyl migration *via* the low-lying **TS3′** furnishes the experimentally obtained 1,1-silaboration product **7**, with an overall reaction energy of $\Delta G = -10.9$ kcal mol^{-1}.

The differing regioselectivities observed in the silaborations of ethylene and cyclohexene arise as early as in intermediates $2 \cdot (C_2H_4)$ and $2 \cdot (C_6H_{10})$: In $2 \cdot (C_2H_4)$, the ethylene coordination is near symmetric with B–C distances of 1.837 and 1.868 Å; the C(2)–C(1)–B–Si torsion angle is 23.0°, which represents an ideal conformation for an ensuing 1,2-silyl shift (Fig. 4a, left). According to a Natural Bond Orbital (NBO) analysis,[128] all three atoms—B, C(1), and C(2)—carry negative partial charges of −0.52, −0.43, and −0.49 e, respectively. Intermediate $2 \cdot (C_2H_4)$ can thus be described as a σ-type donor–acceptor complex, in which charge is transferred from the occupied π-orbital of the olefin to the vacant orbital at the B atom, resulting in a substantial interaction energy of −313 kcal mol^{-1}.[129] Notably,
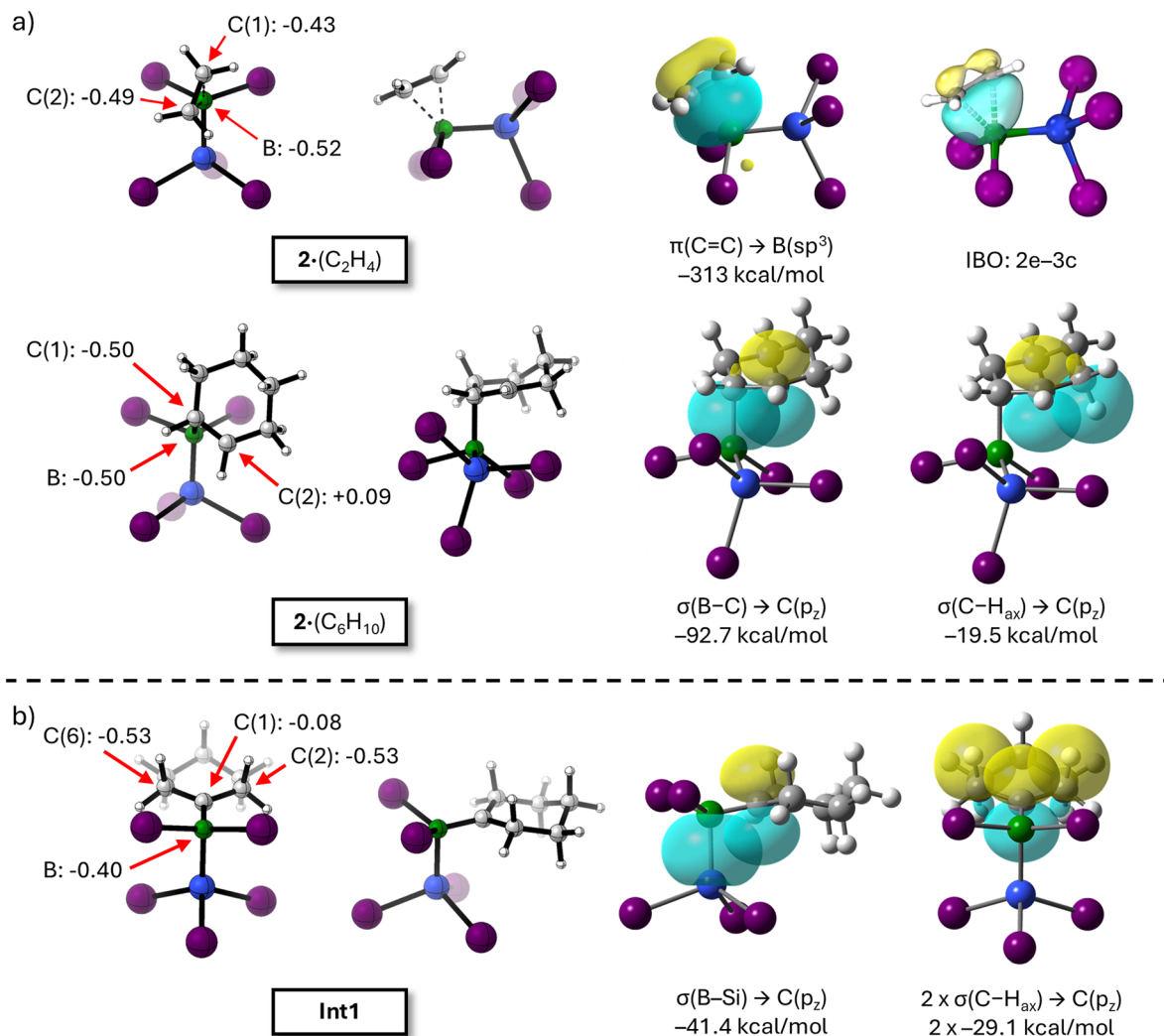
Fig. 4   NBO and IBO analyses rationalizing the divergent silaboration pathways of ethylene and cyclohexene.[129] Color code: H: white, B: green, C: grey, Si: blue, I: violet. (a) Left: optimized structures of $2\cdot(C_2H_4)$ (top) and $2\cdot(C_6H_{10})$ (bottom) with selected NBO charges given in elementary charges (e); right: key orbital interactions with associated stabilization energies; top right: IBO representation of the two-electron–three-center (2e–3c) bond in $2\cdot(C_2H_4)$. (b) Left: Optimized structure of **Int1** with selected NBO charges given in elementary charges (e); right: hyperconjugative interactions stabilizing the carbenium ion, including the β-silicon effect and $C-H_{ax}$ σ donation; SMD(DCM)/PBE0-D3(BJ)/def2-SVPD level of theory.

an Intrinsic Bond Orbital (IBO)[130] analysis even suggests the presence of a C–B–C two-electron–three-center (2e–3c) bond, with relative contributions of 29.4% (B), 35.4% (C(1)), and 34.7% (C(2); Fig. 4a, right). In $2\cdot(C_6H_{10})$, olefin binding is markedly unsymmetric, likely due to the higher steric bulk of cyclohexene relative to ethylene (Fig. 4a, left):[131] a short σ bond is found between the B center and the pyramidalized C(1) atom (1.829 Å), while the distance to the still planar C(2) atom is significantly longer (B⋯C = 2.356 Å). Concomitantly, the torsion angle C(2)–C(1)–B–Si is increased to 52.0°, thereby disfavoring a 1,2-silyl shift due to the longer Si⋯C(2) distance that would have to be traversed in the corresponding transition state. While the NBO charges on B and C(1) in $2\cdot(C_6H_{10})$ remain comparably negative to those in $2\cdot(C_2H_4)$, C(2) now carries a positive charge of +0.09e. Cyclohexene can accommodate the steric constraints, as the carbenium ion at C(2) is stabilized by

both the +I effect of the alkyl substituent and hyperconjugative interactions[132–134] between its vacant p_z orbital and the neighboring B–C and $C-H_{ax}$ σ bonds with contributions worth –92.7 and –19.5 kcal mol^{-1} (ref. 129; Fig. 4a, right; see section 6.3.6 in the SI for a comparison with $3\cdot(C_6H_{10})$ where an NBO analysis reveals that **3** is coordinated primarily through a conventional, symmetric π→B interaction, most likely reflecting the lower Lewis acidity of **3**). Similar hyperconjugative interactions as described for $2\cdot(C_6H_{10})$ are also present in the rearrangement intermediate **Int1**—this time between the carbenium ion's p_z orbital and the B–Si σ bond or two equivalent $C-H_{ax}$ σ bonds (relative energy contributions: –41.4 and 2 × –29.1 kcal mol^{-1}, respectively; Fig. 4b, right). The former interaction corresponds to the well-known β-effect of a silyl group.[125] The overall stabilizing influence of steric and electronic factors makes **Int1** thermodynamically more favorable than $2\cdot(C_6H_{10})$. In

summary, the distinct regioselectivities in ethylene and cyclohexene silaboration originate from substrate-dependent binding geometries to **2**: symmetric coordination of ethylene facilitates direct 1,2-silaboration, whereas the unsymmetric activation of cyclohexene favors a stepwise 1,1-pathway *via* a stabilized carbenium-ion intermediate. The computed energy profiles and bonding analyses offer a coherent explanation for the experimentally observed selectivities and underscore the critical influence of steric and electronic substrate effects in directing the specific silaboration pathway.

Conclusions

The addition of a reactant X–Y across a C=C double bond is a perfectly atom-economic transformation. When employing versatile (orthogonal) functional groups for X and Y, the primary addition products can be made valuable platforms for a wide range of applications. This is particularly true for X–Y-type reactants featuring covalently bonded boryl and silyl groups: both substituents are not only among the most versatile handles for downstream functionalization, but also play key roles as property-defining units in organic functional materials. Consequently, there is a growing demand for the development of novel silaboration reactions and tailored silylborane reagents $R_2B–SiR_3$. We have now found a way to make perhalogenated derivatives (R = Cl, I) readily accessible on a multigram scale—both as free Lewis acids (*e.g.*, $Cl_2B–SiCl_3$) and as Lewis base adducts (Do·$R_2B–SiR_3$; Do = SMe_2, Py, PPh_3, IDipp). These developments create a versatile platform with the following key features: (i) $Me_2S·I_2B–SiI_3$ and the *in situ*-generated mixture $Li[I_3B–SiI_3]/I_2B–SiI_3/LiI$ react directly with olefins in silaboration reactions without the need for a catalyst, which is virtually without precedent.[135] (ii) Cyclohexene undergoes a 1,1-addition reaction—so far unobserved not only for silaborations, but also for diboration and disilylation reactions. Combined experimental and quantum-chemical studies revealed that the steric demand of cyclohexene renders symmetrical coordination of the olefin to the B site unfavorable and instead promotes the formation of a zwitterionic $B^{\ominus}(sp^3)–C(sp^3)–C^{\oplus}(sp^2)$ fragment as a key entry point for the 1,1-silaboration cascade. While such a motif is prohibitively high in energy for ethylene, the carbenium center in the zwitterionic cyclohexene intermediate is efficiently stabilized through a combination of positive inductive (+I) and hyperconjugative effects. (iii) The halide substituents on the introduced boryl and silyl units enable diverse late-stage derivatizations—an aspect of particular importance when these functional groups are not merely used for transmetallation purposes in C–C-coupling reactions, but are instead retained as property-defining elements in the final molecule. (iv) Bulk $Cl_2B–SiCl_3$ can be distilled without decomposition. Considering that Si_2Cl_6 has been successfully used for the gas-phase deposition of silicon thin films,[136] and B_2F_4 for their boron doping,[137,138] $Cl_2B–SiCl_3$ emerges as a promising single-source precursor for semiconductor fabrication. Taken together, these findings pave the way for the future utilization of perhalogenated silylboranes in both synthesis (i–iii) and materials science (iv).

Author contributions

J. H. performed the experimental studies and characterized all new compounds. C. D. B. performed the quantum-chemical calculations. A. V. V. and E. P. performed the X-ray crystal structure analyses of all compounds. H.-W. L., F. F. and M. W. supervised the project. The manuscript was written by J. H., C. D. B. and M. W. and edited by all co-authors.

Conflicts of interest

There are no conflicts to declare.

Data availability

CCDC 2470869, 2470870, 2470871, 2470872, 2470873, 2470874, 2470875, 2470876, 2470877, 2470878, 2470879, 2470880, 2470881, 2470882, 2470883, 2470884, 2470885, 2470886, 2470887, 2470888, and 2470889, contain the supplementary crystallographic data for this paper.[139a–u]

The data supporting this article have been included as part of the SI. Supplementary information is available. See DOI: **https://doi.org/10.1039/d5sc06234a**.

Acknowledgements

Notes and references

1 S. A. Westcott and E. Fernández, in *Adv. Organometal. Chem.*, Academic Press, Cambridge, 2015, vol. 63, pp. 39–89.

2 H. Braunschweig and R. D. Dewhurst, Single, Double, Triple Bonds and Chains: The Formation of Electron-Precise B–B Bonds, *Angew. Chem. Int. Ed.*, 2013, **52**, 3574–3583.

3 R. D. Dewhurst, E. C. Neeve, H. Braunschweig and T. B. Marder, sp^2-sp^3 diboranes: astounding structural variability and mild sources of nucleophilic boron for organic synthesis, *Chem. Commun.*, 2015, **51**, 9594–9607.

4 M. Arrowsmith, H. Braunschweig and T. E. Stennett, Formation and Reactivity of Electron-Precise B-B Single and Multiple Bonds, *Angew. Chem., Int. Ed.*, 2017, **56**, 96–115.

5 M. Arrowsmith, J. Böhnke, H. Braunschweig, A. Deißenberger, R. D. Dewhurst, W. C. Ewing, C. Hörl, J. Mies and J. H. Muessig, Simple solution-phase syntheses of tetrahalodiboranes(4) and their labile dimethylsulfide adducts, *Chem. Commun.*, 2017, **53**, 8265–8267.

6 J. Teichmann and M. Wagner, Silicon chemistry in zero to three dimensions: from dichlorosilylene to silafullerane, *Chem. Commun.*, 2018, **54**, 1397–1412.

7 J. A. Morrison, Chemistry of the Polyhedral Boron Halides and the Diboron Tetrahalides, *Chem. Rev.*, 1991, **91**, 35–48.

8 T. B. Marder and N. C. Norman, Transition metal catalysed diboration, *Top. Catal.*, 1998, **5**, 63–73.

9 Y. J. Lin, C. H. Liu, M. G. Chin, C. C. Wang, S. H. Wang, H. Y. Tsai, J. R. Chen, E. Y. Ngai and R. Ramachandran, Characterization of Shock-Sensitive Deposits from the Hydrolysis of Hexachlorodisilane, *ACS Omega*, 2019, **4**, 1416–1424.

10 Y. J. Lin, T. T. Nguyen, M. G. Chin, C. C. Wang, C. H. Liu, H. Y. Tsai, J. R. Chen, E. Y. Ngai and R. Ramachandran, Disposal of hexachlorodisilane and its hydrolyzed deposits, *J. Loss Prev. Proc. Ind.*, 2020, **65**, 104136.

11 G. Urry, J. Kerrigan, T. D. Parsons and H. I. Schlesinger, Diboron Tetrachloride, B₂Cl₄, as a Reagent for the Synthesis of Organo-boron Compounds. I. The Reaction of Diboron Tetrachloride with Ethylene, *J. Am. Chem. Soc.*, 1954, **76**, 5299–5301.

12 P. Ceron, A. Finch, J. Frey, J. Kerrigan, T. Parsons, G. Urry and H. I. Schlesinger, Diboron Tetrachloride and Tetrafluoride as Reagents for the Synthesis of Organoboron Compounds. II. The Behavior of the Diboron Tetrahalides toward Unsaturated Organic Compounds, *J. Am. Chem. Soc.*, 1959, **81**, 6368–6371.

13 T. Wartik and W. B. Fox, Reaction of Diboron Tetrachloride with Aromatic Substances, *J. Am. Chem. Soc.*, 1961, **83**, 498–499.

14 J. Feeney, A. K. Holliday and F. J. Marsden, Diboron Tetrachloride–Olefin Compounds. Part III. The Reaction of Diboron Tetrachloride with Trichloroethylene, Isobutene, and *cis-* and *trans-*But-2-ene, *J. Chem. Soc.*, 1961, 356–360.

15 M. Zeldin and A. Rosen, The Chemistry of Tetrachlorodiborane(4): I. Reactions with Cyclic Olefins, *J. Organomet. Chem.*, 1971, **31**, 319–328.

16 M. Zeldin and A. Rosen, The Chemistry of Tetrachlorodiborane(4): II. Reactions with Saturated Ring Hydrocarbons, *J. Organomet. Chem.*, 1972, **34**, 259–268.

17 W. Siebert, M. Hildenbrand, P. Hornbach, G. Karger and H. Pritzkow, 1,2- und 1,1-Diborylalkene, *Z. Naturforsch. B*, 1989, **44**, 1179–1186.

18 J. Tillmann, L. Meyer, J. I. Schweizer, M. Bolte, H.-W. Lerner, M. Wagner and M. C. Holthausen, Chloride-Induced Aufbau of Perchlorinated Cyclohexasilanes from Si₂Cl₆: A Mechanistic Scenario, *Chem. Eur. J.*, 2014, **20**, 9234–9239.

19 J. Teichmann, M. Bursch, B. Köstler, M. Bolte, H.-W. Lerner, S. Grimme and M. Wagner, Trapping Experiments on a Trichlorosilanide Anion: a Key Intermediate of Halogenosilane Chemistry, *Inorg. Chem.*, 2017, **56**, 8683–8688.

20 E. C. Neeve, S. J. Geier, I. A. I. Mkhalid, S. A. Westcott and T. B. Marder, Diboron(4) Compounds: From Structural Curiosity to Synthetic Workhorse, *Chem. Rev.*, 2016, **116**, 9091–9161.

21 J. Takaya and N. Iwasawa, Catalytic, Direct Synthesis of Bis(boronate) Compounds, *ACS Catal.*, 2012, **2**, 1993–2006.

22 I. A. I. Mkhalid, J. H. Barnard, T. B. Marder, J. M. Murphy and J. F. Hartwig, C–H Activation for the Construction of C–B Bonds, *Chem. Rev.*, 2010, **110**, 890–931.

23 M. Hildenbrand, H. Pritzkow, U. Zenneck and W. Siebert, Synthesis and Structure of a 1,3-Dihydro-1,3-diborete, *Angew. Chem. Int. Ed. Engl.*, 1984, **23**, 371–372.

24 P. Hornbach, M. Hildenbrand, H. Pritzkow and W. Siebert, A Puckered and a Planar 1,3-Diboretane, *Angew. Chem. Int. Ed. Engl.*, 1986, **25**, 1112–1114.

25 H. Braunschweig, R. D. Dewhurst, K. Hammond, J. Mies, K. Radacki and A. Vargas, Ambient-Temperature Isolation of a Compound with a Boron-Boron Triple Bond, *Science*, 2012, **336**, 1420–1422.

26 J. Böhnke, H. Braunschweig, W. C. Ewing, C. Hörl, T. Kramer, I. Krummenacher, J. Mies and A. Vargas, Diborabutatriene: An Electron-Deficient Cumulene, *Angew. Chem. Int. Ed.*, 2014, **53**, 9082–9085.

27 J. Böhnke, H. Braunschweig, T. Dellermann, W. C. Ewing, K. Hammond, J. O. C. Jimenez-Halla, T. Kramer and J. Mies, The Synthesis of B₂(SIDip)₂ and its Reactivity Between the Diboracumulenic and Diborynic Extremes, *Angew. Chem. Int. Ed.*, 2015, **54**, 13801–13805.

28 H. Braunschweig, S. Demeshko, W. C. Ewing, I. Krummenacher, B. B. Macha, J. D. Mattock, F. Meyer, J. Mies, M. Schäfer and A. Vargas, A Binuclear 1,1'-Bis(boratabenzene) Complex: Unprecedented Intramolecular Metal–Metal Communication through a B–B Bond, *Angew. Chem. Int. Ed.*, 2016, **55**, 7708–7711.

29 W. Lu, Y. Li, R. Ganguly and R. Kinjo, Alkene–Carbene Isomerization induced by Borane: Access to an Asymmetrical Diborene, *J. Am. Chem. Soc.*, 2017, **139**, 5047–5050.

30 G. Urry, Systematic Synthesis in the Polysilane Series, *Acc. Chem. Res.*, 1970, **3**, 306–312.

31 J. I. Schweizer, M. G. Scheibel, M. Diefenbach, F. Neumeyer, C. Würtele, N. Kulminskaya, R. Linser, N. Auner, S. Schneider and M. C. Holthausen, A Disilene Base Adduct with a Dative Si–Si Single Bond, *Angew. Chem. Int. Ed.*, 2016, **55**, 1782–1786.

32 C. Kunkel, M. Bolte, H.-W. Lerner, P. Albert and M. Wagner, Subvalent mixed SiₓGeᵧ oligomers: (Cl₃Si)₄Ge and Cl₂(Me₂EtN)SiGe(SiCl₃)₂, *Chem. Commun.*, 2021, **57**, 12028–12031.

33 I. Georg, J. Teichmann, M. Bursch, J. Tillmann, B. Endeward, M. Bolte, H.-W. Lerner, S. Grimme and M. Wagner, Exhaustively Trichlorosilylated C₁ and C₂ Building Blocks: Beyond the Müller–Rochow Direct Process, *J. Am. Chem. Soc.*, 2018, **140**, 9696–9708.

34 I. Georg, M. Bursch, J. B. Stückrath, E. Alig, M. Bolte, H.-W. Lerner, S. Grimme and M. Wagner, Building up Strain in One Step: Synthesis of an Edge-Fused Double Silacyclobutene from an Extensively Trichlorosilylated Butadiene Dianion, *Angew. Chem. Int. Ed.*, 2020, **59**, 16181–16187.

35 I. Georg, M. Bursch, B. Endeward, M. Bolte, H.-W. Lerner, S. Grimme and M. Wagner, The power of trichlorosilylation: isolable trisilylated allyl anions, allyl

radicals, and allenyl anions, *Chem. Sci.*, 2021, **12**, 12419–12428.

36 M. Schmidt, J. Gilmer, A. Virovets, M. Bolte, H.-W. Lerner and M. Wagner, Adjusting the Number of Functional Groups in Vicinal Bis(trichlorosilylated) Benzenes, *Chem. Eur. J.*, 2024, **30**, e202402998.

37 J. Tillmann, M. Moxter, M. Bolte, H.-W. Lerner and M. Wagner, Lewis Acidity of Si_6Cl_{12} and Its Role as Convenient $SiCl_2$ Source, *Inorg. Chem.*, 2015, **54**, 9611–9618.

38 J. Teichmann, B. Köstler, J. Tillmann, M. Moxter, R. Kupec, M. Bolte, H.-W. Lerner and M. Wagner, Halide-Ion Diadducts of Perhalogenated Cyclopenta- and Cyclohexasilanes, *Z. Anorg. Allg. Chem.*, 2018, **644**, 956–962.

39 J. Teichmann, C. Kunkel, I. Georg, M. Moxter, T. Santowski, M. Bolte, H.-W. Lerner, S. Bade and M. Wagner, Tris(trichlorosilyl)tetrelide Anions and a Comparative Study of Their Donor Qualities, *Chem. Eur. J.*, 2019, **25**, 2740–2744.

40 B. Köstler, H. Bae, J. Gilmer, A. Virovets, H.-W. Lerner, P. Albert, F. Fantuzzi and M. Wagner, Dope it with germanium: selective access to functionalized Si_5Ge heterocycles, *Chem. Commun.*, 2023, **59**, 716–719.

41 B. Köstler, F. Jungwirth, L. Achenbach, M. Sistani, M. Bolte, H.-W. Lerner, P. Albert, M. Wagner and S. Barth, Mixed-Substituted Single-Source Precursors for $Si_{1-x}Ge_x$ Thin Film Deposition, *Inorg. Chem.*, 2022, **61**, 17248–17255.

42 R. Behrle, V. Krause, M. S. Seifner, B. Köstler, K. A. Dick, M. Wagner, M. Sistani and S. Barth, Electrical and Structural Properties of $Si_{1-x}Ge_x$ Nanowires Prepared from a Single-Source Precursor, *Nanomaterials*, 2023, **13**, 627.

43 J. Tillmann, J. H. Wender, U. Bahr, M. Bolte, H.-W. Lerner, M. C. Holthausen and M. Wagner, One-Step Synthesis of a [20]Silafullerane with an Endohedral Chloride Ion, *Angew. Chem. Int. Ed.*, 2015, **54**, 5429–5433.

44 B. Köstler, M. Bolte, H.-W. Lerner and M. Wagner, Selective One-Pot Syntheses of Mixed Silicon-Germanium Heteroadamantane Clusters, *Chem. Eur. J.*, 2021, **27**, 14401–14404.

45 M. Bamberg, M. Bursch, A. Hansen, M. Brandl, G. Sentis, L. Kunze, M. Bolte, H.-W. Lerner, S. Grimme and M. Wagner, $[Cl@Si_{20}H_{20}]^-$: Parent Siladodecahedrane with Endohedral Chloride Ion, *J. Am. Chem. Soc.*, 2021, **143**, 10865–10871.

46 M. Bamberg, T. Gasevic, M. Bolte, A. Virovets, H.-W. Lerner, S. Grimme, M. Bursch and M. Wagner, Brominated [20]silafulleranes: pushing the limits of steric loading, *Chem. Commun.*, 2023, **59**, 7459–7462.

47 M. Bamberg, T. Gasevic, M. Bolte, A. Virovets, H.-W. Lerner, S. Grimme, M. Bursch and M. Wagner, Regioselective Derivatization of Silylated [20]Silafulleranes, *J. Am. Chem. Soc.*, 2023, **145**, 11440–11448.

48 B. Köstler, J. Gilmer, M. Bolte, A. Virovets, H.-W. Lerner, P. Albert, F. Fantuzzi and M. Wagner, Group IV heteroadamantanes: synthesis of Si_6Sn_4 and site-selective derivatization of Si_6Ge_4, *Chem. Commun.*, 2023, **59**, 2295–2298.

49 S. Kühn, B. Köstler, C. True, L. Albers, M. Wagner, T. Müller and C. Marschner, Selective synthesis of germasila-adamantanes through germanium–silicon shift processes, *Chem. Sci.*, 2023, **14**, 8956–8961.

50 T. Gasevic, M. Bamberg, J. Wicke, M. Bolte, A. Virovets, H.-W. Lerner, S. Grimme, A. Hansen, M. Wagner and M. Bursch, Confined Lewis Pairs: Investigation of the $X^- \rightarrow Si_{20}$ Interaction in Halogen-Encapsulating Silafulleranes, *Angew. Chem. Int. Ed.*, 2024, **63**, e202314238.

51 F. Raaii and M. S. Gordon, Potential Energy Surfaces for the Bis-Silylation of Ethylene, *J. Phys. Chem. A*, 1998, **102**, 4666–4668.

52 Y. Alexeev and M. S. Gordon, Theoretical Study of the Bis-Silylation Reaction of Ethylene Catalyzed by Titanium Dichloride, *Organometallics*, 2003, **22**, 4111–4117.

53 D. G. Hall, *Boronic Acids: Preparation and Applications in Organic Synthesis, Medicine and Materials*, Wiley-VCH, Weinheim, 2011.

54 J. W. B. Fyfe and A. J. B. Watson, Recent Developments in Organoboron Chemistry: Old Dogs, New Tricks, *Chem*, 2017, **3**, 31–55.

55 T. Hiyama and M. Oestreich, *Organosilicon Chemistry: Novel Approaches and Reactions*, Wiley-VCH, Weinheim, 2019.

56 J. J. Feng, W. Mao, L. Zhang and M. Oestreich, Activation of the Si–B interelement bond related to catalysis, *Chem. Soc. Rev.*, 2021, **50**, 2010–2073.

57 M. Oestreich, E. Hartmann and M. Mewald, Activation of the Si–B Interelement Bond: Mechanism, Catalysis, and Synthesis, *Chem. Rev.*, 2013, **113**, 402–441.

58 T. Ohmura and M. Suginome, Silylboranes as New Tools in Organic Synthesis, *Bull. Chem. Soc. Jpn.*, 2009, **82**, 29–49.

59 R. Koyanagi, M. Tanaka, Y. Nonaka, K. Mori, S. Morisako, Y. Yamamoto and A. Kawachi, Preparation and Reactions of (Hydrosilyl)diarylborane, *Eur. J. Inorg. Chem.*, 2025, **28**, e202500068.

60 R. Takahashi, J. Jiang, S. Maeda and H. Ito, Introducing Steric Bulk into Silylboranes: Enhanced Bench Stability and Novel Chemical Reactivity, *Angew. Chem. Int. Ed.*, 2025, e202506194.

61 M. Suginome, H. Nakamura and Y. Ito, Platinum-Catalyzed Regioselective Silaboration of Alkenes, *Angew. Chem. Int. Ed. Engl.*, 1997, **36**, 2516–2518.

62 M. Suginome, T. Matsuda, T. Yoshimoto and Y. Ito, Stereoselective 1,4-silaboration of 1,3-dienes catalyzed by nickel complexes, *Org. Lett.*, 1999, **1**, 1567–1569.

63 G. Durieux, M. Gerdin, C. Moberg and A. Jutand, Rate and Mechanism of the Oxidative Addition of a Silylborane to Pt^0 Complexes – Mechanism for the Pt-Catalyzed Silaboration of 1,3-Cyclohexadiene, *Eur. J. Inorg. Chem.*, 2008, 4236–4241.

64 M. Suginome, H. Nakamura and Y. Ito, Regio- and stereo-selective silaboration of alkynes catalysed by palladium and platinum complexes, *Chem. Commun.*, 1996, 2777–2778.

65 S.-y. Onozawa, Y. Hatanaka and M. Tanaka, Palladium-catalysed borylsilylation of alkynes and borylsilylative

carbocyclization of diynes and an enyne compound, *Chem. Commun.*, 1997, 1229–1230.

66 M. Suginome, T. Matsuda and Y. Ito, Nickel-Catalyzed Silaborative Dimerization of Alkynes, *Organometallics*, 1998, **17**, 5233–5235.

67 M. Suginome, T. Matsuda, H. Nakamura and Y. Ito, Regio- and Stereoselective Synthesis of (Z)-β-Silylalkenylboranes by Silaboration of Alkynes Catalyzed by Palladium and Platinum Complexes, *Tetrahedron*, 1999, **55**, 8787–8800.

68 T. Sagawa, Y. Asano and F. Ozawa, Synthesis and Reactions of *cis*-Silyl(boryl)platinum(II) Complexes, *Organometallics*, 2002, **21**, 5879–5886.

69 T. Ohmura, K. Oshima and M. Suginome, Palladium-catalysed *cis*- and *trans*-silaboration of terminal alkynes: complementary access to stereo-defined trisubstituted alkenes, *Chem. Commun.*, 2008, 1416–1418.

70 T. Ohmura, K. Oshima, H. Taniguchi and M. Suginome, Switch of Regioselectivity in Palladium-Catalyzed Silaboration of Terminal Alkynes by Ligand-Dependent Control of Reductive Elimination, *J. Am. Chem. Soc.*, 2010, **132**, 12194–12196.

71 M. B. Ansell, J. Spencer and O. Navarro, (N-Heterocyclic Carbene)₂-Pd(0)-Catalyzed Silaboration of Internal and Terminal Alkynes: Scope and Mechanistic Studies, *ACS Catal.*, 2016, **6**, 2192–2196.

72 M. Zhao, C.-C. Shan, Z.-L. Wang, C. Yang, Y. Fu and Y.-H. Xu, Ligand-Dependent-Controlled Copper-Catalyzed Regio- and Stereoselective Silaboration of Alkynes, *Org. Lett.*, 2019, **21**, 6016–6020.

73 H. Ito, Y. Horita and E. Yamamoto, Potassium *tert*-butoxide-mediated regioselective silaboration of aromatic alkenes, *Chem. Commun.*, 2012, **48**, 8006–8008.

74 E. Yamamoto, R. Shishido, T. Seki and H. Ito, Tris(trimethylsilyl)silylboronate Esters: Novel Bulky, Air- and Moisture-Stable Silylboronate Ester Reagents for Boryl Substitution and Silaboration Reactions, *Organometallics*, 2017, **36**, 3019–3022.

75 Y. Gu, Y. Duan, Y. Shen and R. Martin, Stereoselective Base-Catalyzed 1,1-Silaboration of Terminal Alkynes, *Angew. Chem. Int. Ed.*, 2020, **59**, 2061–2065.

76 K. Nagao, H. Ohmiya and M. Sawamura, *Anti*-Selective Vicinal Silaboration and Diboration of Alkynoates through Phosphine Organocatalysis, *Org. Lett.*, 2015, **17**, 1304–1307.

77 K. Oshima, K. Kurotobi, M. Suginome, Y. Takano, T. Umeyama and H. Imahori, Dearomatizing conversion of pyrazines to 1,4-dihydropyrazine derivatives *via* transition-metal-free diboration, silaboration, and hydroboration, *Chem. Commun.*, 2012, **48**, 8571–8573.

78 Y. Morimasa, K. Kabasawa, T. Ohmura and M. Suginome, Pyridine-Based Organocatalysts for Regioselective *syn*-1,2-Silaboration of Terminal Alkynes and Allenes, *Asian J. Org. Chem.*, 2019, **8**, 1092–1096.

79 E. Yamamoto, K. Izumi, Y. Horita and H. Ito, Anomalous Reactivity of Silylborane: Transition-Metal-Free Boryl Substitution of Aryl, Alkenyl, and Alkyl Halides with Silylborane/Alkoxy Base Systems, *J. Am. Chem. Soc.*, 2012, **134**, 19997–20000.

80 E. Yamamoto, K. Izumi, Y. Horita, S. Ukigai and H. Ito, Formal Nucleophilic Boryl Substitution of Organic Halides with Silylborane/Alkoxy Base System, *Top. Catal.*, 2014, **57**, 940–945.

81 E. Yamamoto, S. Ukigai and H. Ito, Boryl substitution of functionalized aryl-, heteroaryl- and alkenyl halides with silylborane and an alkoxy base: expanded scope and mechanistic studies, *Chem. Sci.*, 2015, **6**, 2943–2951.

82 R. Uematsu, E. Yamamoto, S. Maeda, H. Ito and T. Taketsugu, Reaction Mechanism of the Anomalous Formal Nucleophilic Borylation of Organic Halides with Silylborane: Combined Theoretical and Experimental Studies, *J. Am. Chem. Soc.*, 2015, **137**, 4090–4099.

83 E. Yamamoto, K. Izumi, R. Shishido, T. Seki, N. Tokodai and H. Ito, Direct Introduction of a Dimesitylboryl Group Using Base-Mediated Substitution of Aryl Halides with Silyldimesitylborane, *Chem. Eur. J.*, 2016, **22**, 17547–17551.

84 E. Yamamoto, S. Maeda, T. Taketsugu and H. Ito, Transition-Metal-Free Boryl Substitution Using Silylboranes and Alkoxy Bases, *Synlett*, 2017, **28**, 1258–1267.

85 J. M. O'Brien and A. H. Hoveyda, Metal-Free Catalytic C–Si Bond Formation in an Aqueous Medium. Enantioselective NHC-catalyzed Silyl Conjugate Additions to Cyclic and Acyclic α,β-Unsaturated Carbonyls, *J. Am. Chem. Soc.*, 2011, **133**, 7712–7715.

86 C. Kleeberg and C. Borner, On the Reactivity of Silylboranes toward Lewis Bases: Heterolytic B–Si Cleavage vs. Adduct Formation, *Eur. J. Inorg. Chem.*, 2013, 2799–2806.

87 C. Kleeberg, On the structural diversity of [K(18-crown-6) EPh₃] complexes (E = C, Si, Ge, Sn, Pb): Synthesis, crystal structures and NOESY NMR study, *Dalton Trans.*, 2013, **42**, 8276–8287.

88 J. Plotzitzka and C. Kleeberg, [(NHC)Cuᴵ–ER₃] Complexes (ER₃ = SiMe₂Ph, SiPh₃, SnMe₃): From Linear, Mononuclear Complexes to Polynuclear Complexes with Ultrashort Cuᴵ···Cuᴵ Distances, *Inorg. Chem.*, 2016, **55**, 4813–4823.

89 J. Plotzitzka and C. Kleeberg, [(18-C-6)K][(N≡C)Cuᴵ–SiMe₂Ph], a Potassium Silylcyanocuprate as a Catalyst Model for Silylation Reactions with Silylboranes: Syntheses, Structures, and Catalytic Properties, *Inorg. Chem.*, 2017, **56**, 6671–6680.

90 P. Gao, G. Wang, L. Xi, M. Wang, S. Li and Z. Shi, Transition-Metal-Free Defluorosilylation of Fluoroalkenes with Silylboronates, *Chin. J. Chem.*, 2019, **37**, 1009–1014.

91 R. Shishido, M. Uesugi, R. Takahashi, T. Mita, T. Ishiyama, K. Kubota and H. Ito, General Synthesis of Trialkyl- and Dialkylarylsilylboranes: Versatile Silicon Nucleophiles in Organic Synthesis, *J. Am. Chem. Soc.*, 2020, **142**, 14125–14133.

92 A. B. Cuenca, R. Shishido, H. Ito and E. Fernández, Transition-metal-free B–B and B–interelement reactions with organic molecules, *Chem. Soc. Rev.*, 2017, **46**, 415–430.

93 J. Gilmer, M. Bolte, A. Virovets, H.-W. Lerner, F. Fantuzzi and M. Wagner, A Hydride-Substituted Homoleptic Silylborate: How Similar is it to its Diborane(6)-Dianion Isostere?, *Chem. Eur. J.*, 2023, **29**, e202203119.

94 J. Gilmer, T. Trageser, L. Čaić, A. Virovets, M. Bolte, H.-W. Lerner, F. Fantuzzi and M. Wagner, Catalyst-free diboration and silaboration of alkenes and alkynes using bis(9-heterofluorenyl)s, *Chem. Sci.*, 2023, **14**, 4589–4596.

95 S. Bochmann, U. Böhme, E. Brendler, M. Friebel, M. Gerwig, F. Gründler, B. Günther, E. Kroke, R. Lehnert and L. Ruppel, Unexpected Formation of the Highly Symmetric Borate Ion $[B(SiCl_3)_4]^-$, *Eur. J. Inorg. Chem.*, 2021, 2583–2594.

96 P. Greiwe, A. Bethäuser, H. Pritzkow, T. Kühler, P. Jutzi and W. Siebert, Borane-stabilized Boranediyls (Borylenes): Neutral *nido*-1-Borane-2,3,4,5,6-pentamethyl-2,3,4,5,6-pentacarbahexaboranes(6), *Eur. J. Inorg. Chem.*, 2000, 1927–1929.

97 N. Sen, N. Parvin, S. Tothadi and S. Khan, Reactivity of $(TMS)_2N(\eta^1-Cp^*)Si=Si(\eta^1-Cp^*)N(TMS)_2$ toward the Halides of Groups 13–15, *Organometallics*, 2021, **40**, 1874–1883.

98 A. Stock, A. Brandt and H. Fischer, Der Zink-Lichtbogen als Reduktionsmittel, *Ber. Dtsch. Chem. Ges. B*, 1925, **58**, 643–657.

99 T. Wartik, R. Moore and H. I. Schlesinger, Derivatives of Diborine, *J. Am. Chem. Soc.*, 1949, **71**, 3265–3266.

100 G. Urry, T. Wartik, R. E. Moore and H. I. Schlesinger, The Preparation and Some of the Properties of Diboron Tetrachloride, B_2Cl_4, *J. Am. Chem. Soc.*, 1954, **76**, 5293–5298.

101 H. Nöth and H. Pommerening, Eine einfache Synthese von Dibortetrabromid, *Chem. Ber.*, 1981, **114**, 398–399.

102 X. Zhou, M. A. Wanous, X. Wang, D. V. Eldred and T. L. Sanders, Study on the Shock Sensitivity of the Hydrolysis Products of Hexachlorodisilane, *Ind. Eng. Chem. Res.*, 2018, **57**, 10354–10364.

103 S. Isomura and K. Takeuchi, Preparation of hexafluorodisilane, *J. Fluorine Chem.*, 1997, **83**, 89–91.

104 M. Berger, N. Auner and M. Bolte, Hexabromo- and hexaiododisilane: small and simple molecules showing completely different crystal structures, *Acta Crystallogr. Sect. C*, 2014, **70**, 1088–1091.

105 I. Krossing, The Facile Preparation of Weakly Coordinating Anions: Structure and Characterisation of Silverpolyfluoroalkoxyaluminates $AgAl(OR_F)_4$, Calculation of the Alkoxide Ion Affinity, *Chem. Eur. J.*, 2001, **7**, 490–502.

106 Alternative syntheses of $Cl_2B–SiCl_3$ have been reported, but are of limited practical use due to the demanding apparatus and low yields: (*a*) A. G. Massey and D. S. Urch, *Proc. Chem. Soc.*, 1964, 273–312: $Cl_2B–SiCl_3$ formed in trace amounts during a mercury discharge of BCl_3 vapor, likely *via* reaction with $SiCl_4$ generated from etching of a quartz discharge tube; (*b*) P. L. Timms, *Inorg. Chem.*, 1968, **7**, 387–389: $SiCl_2$, generated from Si and $SiCl_4$ at high temperature, was cocondensed with BCl_3 (1 : 1) at –196 °C, yielding a blue solid that, upon warming, released $Cl_2B–SiCl_3$; (*c*) R. W. Kirk, D. L. Smith, W. Airey and P. L. Timms, *J. Chem. Soc., Dalton Trans.*, 1972, **13**, 1392–1396: Condensation of $SiCl_2$ with B_2Cl_4 at –196 °C, followed by warming under reduced pressure, produced

a complex, unstable mixture from which only $Cl_2B–SiCl_3$ could be isolated and identified; (*d*) M. Zeldin, D. Solan and B. Dickman, *J. Inorg. Nucl. Chem.*, 1975, **37**, 25–28: Using a $SiCl_4/BCl_3$ gas mixture under electric discharge, $Cl_2B–SiCl_3$ was prepared and isolated in low yield ($\approx 0.2\%$) by fractional condensation and distillation.

107 Deposition Numbers 2470869 (for **2**·IDipp), 2470870 (for **2**·PPh_3 (α-)), 2470871 (for **2**·PPh_3 (β-)), 2470872 (for **2**·Py), 2470873 (for **2**·SMe_2 (α-)), 2470874 (for **2**·SMe_2 (β-)), 2470875 (for **3**·IDipp), 2470876 (for **3**·PPh_3), 2470877 (for **3**·Py), 2470878 (for **3**·SMe_2), 2470879 (for **4**), 2470880 (for **5**·SMe_2), 2470881 (for **5**·Py), 2470882 (for **7** (α-)), 2470883 (for **7** (β-)), 2470884 (for **8**), 2470885 (for $[Et_4N][Cl_3B–SiCl_3]$), 2470886 (for $[Et_4N][(I_{2.03}/Cl_{0.97})B–SiI_3]$), 2470887 (for BI_3·IDipp), 2470888 (for BI_3·PPh_3), and 2470889 (for Me_2S·$I_2B–C_2H_4–I$) contain the supplementary crystallographic data for this paper. These data are provided free of charge by the joint Cambridge Crystallographic Data Centre and Fachinformationszentrum Karlsruhe Access Structures service.

108 H. Nöth and B. Wrackmeyer, Nuclear Magnetic Resonance Spectroscopy of Boron Compounds, in *NMR Basic Principles and Progress*, ed. P. Diehl, E. Fluck and R. Kosfeld, Springer Verlag, Berlin, Heidelberg, New York, 1978.

109 Replacement of *o*DFB with CH_2Cl_2 led to I/Cl exchange, giving rise to CD_2ICl, CD_2I_2, and 1,1-dichloro-3,4-dimethyl-1-silacyclopent-3-ene (GC-MS: Fig. S1), along with $IDipp$·BCl_3 (^{11}B NMR spectroscopy; Fig. S62).

110 **2**·SMe_2 is dimorphic. To confirm the phase purity of a freshly prepared sample of **2**·SMe_2, measured powder diffraction data must be compared with simulated patterns of both polymorphs.

111 The B–Do bonds within each **2**·Do/**3**·Do pair featuring the same ligand tend to be slightly shorter in **2**·Do, *e.g.*, **2**·SMe_2 (B–S = 1.927[2] Å)^a *vs.* **3**·SMe_2 (B–S = 1.959(2) Å). Pyramidalization at boron was assessed by comparing the sum of the three bond angles in each $SiBX_2$ fragment to that of three equivalent angles in an ideal tetrahedron ($\sum = 328.5°$). Almost all B sites in **2**·Do/**3**·Do show equal or even greater pyramidalization [exceptions: β-**2**·SMe_2 ($\sum = 330.3(6)°$) and **3**·SMe_2 ($\sum = 333.1(4)°$)]. Adducts **2**·Do are generally more pyramidalized than **3**·Do, with the strongest donor IDipp producing the most pronounced effect: **2**·IDipp ($\sum = 308.6(5)°$), **3**·IDipp ($\sum = 315.1[4]°$).^{b} (*a*) The average value with standard deviations in square brackets was calculated from the following individual bond lengths: B–S = 1.925(6), 1.927(6) (α-polymorph; two crystallographically unique molecules); 1.930(5) Å (β-polymorph); (*b*) The average value with standard deviations in square brackets was calculated from the bond angles of three crystallographically unique molecules: $\sum = 314.75(54), 314.95(54), 315.65(53)°$.

112 The Si(2)–I bond involving a bridging I atom is clearly longer (2.611(4) Å) than the terminal Si(2)–I bonds (2.428(4)/2.403(4) Å).

113 R. Oshimizu, N. Ando and S. Yamaguchi, Olefin–Borane Interactions in Donor–π–Acceptor Fluorophores that Undergo Frustrated-Lewis-Pair-Type Reactions, *Angew. Chem. Int. Ed.*, 2022, **61**, e202209394.

114 The presence or absence of SMe_2 in the reaction mixture does not appear to be decisive in this context, as the product obtained under SMe_2-free conditions has the same NMR signature after addition of the ligand as the compound formed in the long-term reaction between **2**·SMe_2 and cyclohexene (see the SI for more details).

115 Alternative synthesis routes to 1,1-diboryl- and 1-boryl-1-silylalkanes do exist and the particular synthetic value of such compounds has been emphasized. Selected examples: (*a*) H. Li, X. Shangguan, Z. Zhang, S. Huang, Y. Zhang and J. Wang, *Org. Lett.*, 2014, **16**, 448–451; (*b*) A. Millán, P. D. Grigol Martinez and V. K. Aggarwal, *Chem. Eur. J.*, 2018, **24**, 730–735.

116 J. Guo, M. Yan and D. W. Stephan, Frustrated Lewis pair chemistry of alkynes, *Organic Chemistry Frontiers*, 2024, **11**, 2375–2396.

117 M. A. Dureen, C. C. Brown and D. W. Stephan, Deprotonation and Addition Reactions of Frustrated Lewis Pairs with Alkynes, *Organometallics*, 2010, **29**, 6594–6607.

118 C. A. Tanur and D. W. Stephan, The Thioether–Methyleneborane (PhSCH$_2$B(C$_6$F$_5$)$_2$)$_2$: Synthesis and Reactivity with Donors and Alkynes, *Organometallics*, 2011, **30**, 3652–3657.

119 A. Fukazawa, E. Yamaguchi, E. Ito, H. Yamada, J. Wang, S. Irle and S. Yamaguchi, Zwitterionic Ladder Stilbenes with Phosphonium and Borate Bridges: Intramolecular Cascade Cyclization and Structure–Photophysical Properties Relationship, *Organometallics*, 2011, **30**, 3870–3879.

120 C. Eller, G. Kehr, C. G. Daniliuc, R. Fröhlich and G. Erker, Facile 1,1-Carboboration Reactions of Acetylenic Thioethers, *Organometallics*, 2013, **32**, 384–386.

121 D. J. Faizi, A. J. Davis, F. B. Meany and S. A. Blum, Catalyst-Free Formal Thioboration to Synthesize Borylated Benzothiophenes and Dihydrothiophenes, *Angew. Chem. Int. Ed.*, 2016, **55**, 14286–14290.

122 A. J. Warner, A. Churn, J. S. McGough and M. J. Ingleson, BCl$_3$-Induced Annulative Oxo- and Thioboration for the Formation of C3-Borylated Benzofurans and Benzothiophenes, *Angew. Chem. Int. Ed.*, 2017, **56**, 354–358.

123 K. B. Wiberg, J. D. Hammer, H. Castejon, W. F. Bailey, E. L. DeLeon and R. M. Jarret, Conformational Studies in the Cyclohexane Series. 1. Experimental and Computational Investigation of Methyl, Ethyl, Isopropyl, and *tert*-Butylcyclohexanes, *J. Org. Chem.*, 1999, **64**, 2085–2095.

124 H. M. Pickett and H. L. Strauss, Conformational Structure, Energy, and Inversion Rates of Cyclohexane and Some Related Oxanes, *J. Am. Chem. Soc.*, 1970, **92**, 7281–7290.

125 J. B. Lambert, Y. Zhao, R. W. Emblidge, L. A. Salvador, X. Liu, J. H. So and E. C. Chelius, The β Effect of Silicon and Related Manifestations of σ Conjugation, *Acc. Chem. Res.*, 1999, **32**, 183–190.

126 We have confirmed that the model reactant BI$_3$·SMe$_2$ is competent in the iodoboration of ethylene (see the SI for details).

127 Compared to the computed C=C double-bond lengths of ethylene and cyclohexene, the corresponding distances in the olefin complexes are considerably elongated: (i) 1.332 [C$_2$H$_4$] *vs.* 1.380 Å [**2**·(C$_2$H$_4$)]; (ii) 1.340 [C$_6$H$_{10}$] *vs.* 1.392 Å [**2**·(C$_6$H$_{10}$)].

128 J. P. Foster and F. Weinhold, Natural Hybrid Orbitals, *J. Am. Chem. Soc.*, 1980, **102**, 7211–7218.

129 The second-order perturbation energy E(2) in Natural Bond Orbital (NBO) analysis quantifies the stabilization arising from donor–acceptor interactions between occupied (donor) and unoccupied (acceptor) NBOs. It reflects the energetic benefit of intramolecular electron delocalization but must not be interpreted as a bond dissociation energy or a direct measure of intrinsic bond strength. Rather, E(2) serves as a qualitative indicator of hyperconjugative interactions and other delocalization effects within the electronic structure. Although E(2) values are conventionally reported as positive, we present them as negative throughout the text and figures to emphasize their stabilizing effect.

130 G. Knizia, Intrinsic Atomic Orbitals: An Unbiased Bridge Between Quantum Theory and Chemical Concepts, *J. Chem. Theory Comput.*, 2013, **9**, 4834–4843.

131 This assumption is supported, *inter alia*, by quantum-chemical calculations showing that the cyclohexene in the hypothetical complex **3**·(C$_6$H$_{10}$), with iodine atoms replaced by smaller chlorine atoms, primarily coordinates *via* symmetric π-donation—as observed in **2**·(C$_2$H$_4$); more details are provided in the SI.

132 H. Cohn, E. D. Hughes, M. H. Jones and M. G. Peeling, Effects of Alkyl Groups in Electrophilic Additions and Substitutions, *Nature*, 1952, **169**, 291.

133 I. Fernández and G. Frenking, Hyperconjugative Stabilization in Alkyl Carbocations: Direct Estimate of the β-Effect of Group-14 Elements, *J. Phys. Chem. A*, 2007, **111**, 8028–8035.

134 M. C. Elliott, C. E. Hughes, P. J. Knowles and B. D. Ward, Alkyl groups in organic molecules are NOT inductively electron-releasing, *Org. Biomol. Chem.*, 2025, **23**, 352–359.

135 The only other example reported to date, which requires a unique type of silylborane, is described in ref. 94.

136 Evonik Industries, Bau einer Spezialchemie-Anlage für Elektronikchips gestartet, **https://publications.evonik. com/de/presse/pressemitteilungen/corporate/bau-einer-spezialchemie-anlage-fuer-elektronikchips-gestartet-105329.html**.

137 O. Byl, E. Jones, J. Sweeney and R. Kaim, Properties of Diboron Tetrafluoride (B$_2$F$_4$), a New Gas for Boron Ion Implantation, *AIP Conf. Proc.*, 2011, **1321**, 408–410.

138 Y. Tang, O. Byl, A. Avila, J. Sweeney, R. Ray, J. Koo, M.-S. Jeon, T. Miller, S. Krause, W. Skinner and J. Mullin, High-efficiency, high-productivity boron doping

implantation by diboron tetrafluoride (B₂F₄) gas on Applied Materials solar ion implanter, *20th International Conference on Ion Implantation Technology (IIT)*, DOI: **10.1109/IIT.2014.6939984**.

139 (*a*) J. Heller, C. D. Buch, A. V. Virovets, E. Peresypkina, H.-W. Lerner, F. Fantuzzi and M. Wagner, CCDC 2470869, Experimental Crystal Structure Determination, 2025, DOI: **10.5517/ccdc.csd.cc2ny4g7**; (*b*) J. Heller, C. D. Buch, A. V. Virovets, E. Peresypkina, H.-W. Lerner, F. Fantuzzi and M. Wagner, CCDC 2470870, Experimental Crystal Structure Determination, 2025, DOI: **10.5517/ccdc.csd.cc2ny4h8**; (*c*) J. Heller, C. D. Buch, A. V. Virovets, E. Peresypkina, H.-W. Lerner, F. Fantuzzi and M. Wagner, CCDC 2470871, Experimental Crystal Structure Determination, 2025, DOI: **10.5517/ccdc.csd.cc2ny4j9**; (*d*) J. Heller, C. D. Buch, A. V. Virovets, E. Peresypkina, H.-W. Lerner, F. Fantuzzi and M. Wagner, CCDC 2470872, Experimental Crystal Structure Determination, 2025, DOI: **10.5517/ccdc.csd.cc2ny4kb**; (*e*) J. Heller, C. D. Buch, A. V. Virovets, E. Peresypkina, H.-W. Lerner, F. Fantuzzi and M. Wagner, CCDC 2470873, Experimental Crystal Structure Determination, 2025, DOI: **10.5517/ccdc.csd.cc2ny4lc**; (*f*) J. Heller, C. D. Buch, A. V. Virovets, E. Peresypkina, H.-W. Lerner, F. Fantuzzi and M. Wagner, CCDC 2470874, Experimental Crystal Structure Determination, 2025, DOI: **10.5517/ccdc.csd.cc2ny4md**; (*g*) J. Heller, C. D. Buch, A. V. Virovets, E. Peresypkina, H.-W. Lerner, F. Fantuzzi and M. Wagner, CCDC 2470875, Experimental Crystal Structure Determination, 2025, DOI: **10.5517/ccdc.csd.cc2ny4nf**; (*h*) J. Heller, C. D. Buch, A. V. Virovets, E. Peresypkina, H.-W. Lerner, F. Fantuzzi and M. Wagner, CCDC 2470876, Experimental Crystal Structure Determination, 2025, DOI: **10.5517/ccdc.csd.cc2ny4pg**; (*i*) J. Heller, C. D. Buch, A. V. Virovets, E. Peresypkina, H.-W. Lerner, F. Fantuzzi and M. Wagner, CCDC 2470877, Experimental Crystal Structure Determination, 2025, DOI: **10.5517/ccdc.csd.cc2ny4qh**; (*j*) J. Heller, C. D. Buch, A. V. Virovets, E. Peresypkina, H.-W. Lerner, F. Fantuzzi and M. Wagner, CCDC 2470878, Experimental Crystal Structure Determination, 2025, DOI: **10.5517/ccdc.csd.cc2ny4rj**; (*k*) J. Heller, C. D. Buch, A. V. Virovets, E. Peresypkina, H.-W. Lerner, F. Fantuzzi and M. Wagner, CCDC 2470879, Experimental Crystal Structure Determination, 2025, DOI: **10.5517/ccdc.csd.cc2ny4sk**; (*l*) J. Heller, C. D. Buch, A. V. Virovets, E. Peresypkina, H.-W. Lerner, F. Fantuzzi and M. Wagner, CCDC 2470880, Experimental Crystal Structure Determination, 2025, DOI: **10.5517/ccdc.csd.cc2ny4tl**; (*m*) J. Heller, C. D. Buch, A. V. Virovets, E. Peresypkina, H.-W. Lerner, F. Fantuzzi and M. Wagner, CCDC 2470881, Experimental Crystal Structure Determination, 2025, DOI: **10.5517/ccdc.csd.cc2ny4vm**; (*n*) J. Heller, C. D. Buch, A. V. Virovets, E. Peresypkina, H.-W. Lerner, F. Fantuzzi and M. Wagner, CCDC 2470882, Experimental Crystal Structure Determination, 2025, DOI: **10.5517/ccdc.csd.cc2ny4wn**; (*o*) J. Heller, C. D. Buch, A. V. Virovets, E. Peresypkina, H.-W. Lerner, F. Fantuzzi and M. Wagner, CCDC 2470883, Experimental Crystal Structure Determination, 2025, DOI: **10.5517/ccdc.csd.cc2ny4xp**; (*p*) J. Heller, C. D. Buch, A. V. Virovets, E. Peresypkina, H.-W. Lerner, F. Fantuzzi and M. Wagner, CCDC 2470884, Experimental Crystal Structure Determination, 2025, DOI: **10.5517/ccdc.csd.cc2ny4yq**; (*q*) J. Heller, C. D. Buch, A. V. Virovets, E. Peresypkina, H.-W. Lerner, F. Fantuzzi and M. Wagner, CCDC 2470885, Experimental Crystal Structure Determination, 2025, DOI: **10.5517/ccdc.csd.cc2ny4zr**; (*r*) J. Heller, C. D. Buch, A. V. Virovets, E. Peresypkina, H.-W. Lerner, F. Fantuzzi and M. Wagner, CCDC 2470886, Experimental Crystal Structure Determination, 2025, DOI: **10.5517/ccdc.csd.cc2ny50t**; (*s*) J. Heller, C. D. Buch, A. V. Virovets, E. Peresypkina, H.-W. Lerner, F. Fantuzzi and M. Wagner, CCDC 2470887, Experimental Crystal Structure Determination, 2025, DOI: **10.5517/ccdc.csd.cc2ny51v**; (*t*) J. Heller, C. D. Buch, A. V. Virovets, E. Peresypkina, H.-W. Lerner, F. Fantuzzi and M. Wagner, CCDC 2470888, Experimental Crystal Structure Determination, 2025, DOI: **10.5517/ccdc.csd.cc2ny52w**; (*u*) J. Heller, C. D. Buch, A. V. Virovets, E. Peresypkina, H.-W. Lerner, F. Fantuzzi and M. Wagner, CCDC 2470889, Experimental Crystal Structure Determination, 2025, DOI: **10.5517/ccdc.csd.cc2ny53x.**